

**VISVESVARAYA TECHNOLOGICAL UNIVERSITY (VTU)**  
**JNANA SANGAMA, BELGAVI-590018**  
**BACHELOR OF ENGINEERING**



**DEPARTMENT OF MECHANICAL ENGINEERING**

**A PROJECT REPORT ON**

**“EXPERIMENTAL STUDY TO IMPROVE PERFORMANCE OF COMPLIANT  
FOIL THRUST BEARING”**

**SUBMITTED BY**

<b>SAGAR M S</b>	<b>( 1JS15ME083 )</b>
<b>PAVAN KUMAR N</b>	<b>( 1JS16ME417 )</b>
<b>SRINIVAS H P</b>	<b>( 1JS15ME094 )</b>
<b>HARSHITH M S</b>	<b>( 1JS15ME033 )</b>

**UNDER THE GUIDANCE OF: -**

**Mr. NAGARAJA T K**

Assistant professor

Department of Mechanical Engineering



**J.S.S ACADEMY OF TECHNICAL EDUCATION, BANGALORE -60**

**DEPARTMENT OF MECHANICAL ENGINEERING**

JSSATE-B Campus, Dr. Vishnuvardan Road, Srinivaspura, Bangalore, Karnataka 560060

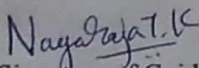
**2019-20**

**JSS ACADEMY OF TECHNICAL EDUCATION**  
JSS CAMPUS, MYLASANDRA, UTTARAHALLI-KENGERI MAIN ROAD,  
BANGALORE-60  
**DEPARTMENT OF MECHANICAL ENGINEERING**

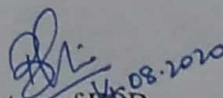


**CERTIFICATE**

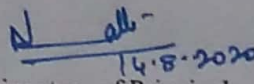
Certified that project entitled **“EXPERIMENTAL STUDY TO IMPROVE PERFORMANCE OF COMPLIANT FOIL THRUST BEARING”** carried out by **Mr. Sagar M S USN:1JS15ME083, Mr. Pavan Kumar N USN:1JS16ME417, Mr. Srinivas H P USN:1JS15ME094 And Mr. Harshith M S USN:1JS15ME033**, bonafied student of JSS Academy of Technical Education Bangalore in Partial Fulfillment for the award of the Bachelor of Engineering in Mechanical Engineering of the Visvesvaraya Technological University, Belgaum during the academic year 2019-2020. It is certified that all the corrections/suggestions indicated of internal assessment have been incorporated in the report. The report has been approved and it satisfies the academic requirement in respect of project work prescribed for the Bachelor of Engineering Degree.

  
Signature of Guide

**Mr. Nagaraja T K**

  
Signature of HOD

**Dr. Bhimasen Soragoan**  
Head of the Department  
Department of Mechanical Engineering  
JSSATE, B-60

  
Signature of Principal

**Dr. Mrityunjaya V. Latte**

**NAME OF EXAMINER**

**SIGNATURE WITH DATE**

- 1.
- 2.
- 3.

## DECLARATION

We, the students of the final semester of Mechanical Engineering, JSS Academy of Technical Education, Bengaluru - 560060 declare that the work entitled **"EXPERIMENTAL STUDY TO IMPROVE PERFORMANCE OF COMPLIANT FOIL THRUST BEARING"** has been completed under the guidance of **Mr. NAGARAJA T K** Assistant Professor, Department of Mechanical Engineering, JSS Academy of Technical Education, Bangalore. This dissertation work is submitted to Visvesvaraya Technological University in partial fulfillment of the requirements for the award of Degree of Bachelor of Engineering in Mechanical Engineering during the academic year 2019-2020. Further, the matter embodied in the project report has not been submitted previously by anybody for the award of any degree or diploma to any university.

Place:

Date:

Team members

1. SAGAR M S

2. PAVAN KUMAR N

3. SRINIVAS H P

4. HARSHITH M S

Signature

The block contains four handwritten signatures. The first signature is for Sagar M S, the second for Pavan Kumar N, the third for Srinivas H P, and the fourth for Harshith M S. There is also a signature of the guide, Mr. Nagaraja T K, at the top of the signature column.

## ACKNOWLEDGMENT

My sincere thanks to the Management of **JSS ACADEMY OF TECHNICAL EDUCATION, BANGALORE** for providing excellent infrastructure and lab facilities that helped me to go through the different areas of interest.

It is my privilege and pleasure to express our profound sense of respect, gratitude, and indebtedness to **Dr. Mrityunjaya V Latte, Principal, JSSATEB**, for providing facilities for the successful completion of the project.

I sincerely thank **Dr. Bhimasen Soragaon, Professor & HOD, Department of Mechanical Engineering, JSSATEB**, for his valuable support and constant encouragement given during this work.

I also thank my guide, **Mr. NAGARAJA T K Assistant Professor, Department of Mechanical Engineering, JSSATEB**, for guiding and for his valuable support and constant encouragement given during this work.

I also thank all the **Staff Members** of the **Department of Mechanical Engineering of JSSATEB** for their cooperation.

Finally, I wish to acknowledge **Parents and Friends** for giving moral strength and encouragement.

## **Abstract**

Foil bearings are self-acting hydrodynamic bearings, which supports lightly loaded shafts with major advantages like physically non-contacting high-speed operation. However, the lack of load-carrying capacity at relatively lower speeds limits their applications in heavy turbomachinery. This project aims to reduce the complexity and improve the load-carrying capability, mechanical efficiency, and stability of high-speed rotating foil thrust bearing. The load carrying capabilities depend on the function of speed, the gap between the bearing and the runner as well as the shape of foils for an airfoil thrust bearing. The effects of various bearing parameters like foil thickness, number of foils fixed, foil geometry, and position of foils along the circumference. Varying these parameters, we can achieve improvement in stability and load-carrying capability. Analysis and Simulations in the software were conducted by changing parameters of bearing by varying the number of foils and changing the type of foil and providing supports to foil to improve the performance of the bearing. Present work discusses the assessment of load-carrying capabilities as a function of speed. Performance characteristics are defined essentially in terms of load-carrying capabilities and Speeds has been evaluated by Software simulation.

## **CONTENTS**

<b>Chapters</b>	<b>Description</b>	<b>Page Number</b>
<b>Chapter 1</b>	<b>INTRODUCTION</b>	<b>1</b>
1.1	Journal Foil bearing	3
1.2	Working of Foil bearing	3
1.3	Types of Air foil bearings	4
1.4	Applications of Air foil bearings	4
1.5	Thrust bearing	5
1.6	Thrust bearings come in several varieties.	5
1.7	Fluid bearing	7
1.8	Hydrodynamic bearing	7
1.9	Thrust Foil Bearing	6
1.10	Working of Thrust Foil Bearing	8
1.11	Pressure Development in Air Foil Thrust Bearing	8
1.12	History	9
1.13	Applications	10
1.14	Advantages	10
1.15	Disadvantages	11
<b>Chapter 2</b>	<b>LITERATURE SURVEY</b>	<b>12</b>
<b>Chapter 3</b>	<b>OUTCOMES OF LITERATURE SURVEY</b>	<b>21</b>
<b>Chapter 4</b>	<b>PROBLEM DEFINITION</b>	<b>23</b>
<b>Chapter 5</b>	<b>OBJECTIVES</b>	<b>25</b>
<b>Chapter 6</b>	<b>METHODOLOGY</b>	<b>27</b>

<b>Chapter 7</b>	<b>DESIGN ASPECTS AND FABRICATION</b>	<b>29</b>
7.1	CAD Model of Thrust Runner	30
7.2	CAD Model of Bearing Block	30
7.3	Different Sector Angles of Foils	31
7.4	3D CAD Model of the Bearing block and runner	32
7.5	Runner and Bearing block with foil assembly	33
7.6	Fabrication	33
<b>Chapter 8</b>	<b>FLUID STRUCTURE INTERACTION SIMULATION</b>	<b>34</b>
<b>Chapter 9</b>	<b>FSI SIMULATION RESULTS</b>	<b>41</b>
9.1	Different Sector Angle configurations	42
9.2	Different Foil Thickness configurations	45
9.3	Viscoelastic Support configuration	51
<b>Chapter 10</b>	<b>RESULTS AND DISCUSSION</b>	<b>57</b>
<b>Chapter 11</b>	<b>CONCLUSION</b>	<b>60</b>
<b>Chapter 12</b>	<b>REFERENCES</b>	<b>62</b>

## LIST OF FIGURES

Figure Number	Description	Page Number
1	Journal Foil Bearing [20]	3
2	Thrust Ball Bearing [21]	5
3	Thrust Foil Bearing [22]	7
4	Thrust foil bearing principle of working [23]	8
5	Methodology Flow Chart	28
6	2D Model of Thrust Runner	30
7	2D Model of Bearing Block	31
8	2D Model of 3 Different Sector Angle of Foils and a support Shim	31
9	3D CAD Model and Assembly of Foils to Bearing Block	32
10	3D CAD Model of Runner	32
11	3D CAD Model Assembly of Bearing Block, Runner, and 90 Degree Sector angle Foils	33
12	Parameters and equations Table	35
13	Air Duct (Boundary Wall) geometry	35
14	Shim geometry	36
15	Foil Sector angle geometry	36
16	List of FSI Property Selection and Complete 3D Model Ready for Meshing	37
17	Meshed Model	37
18	Stress Distribution and Air Flow	38
19	Pressure Contour	38
20	Stress Distribution due to Pressure on 90-degree foil surface	39
21	Stress Distribution due to Pressure on Runner surface	39
22	Displacement / Deflection of 90-degree sector angle foil	40
23	Stress Distribution due to Pressure of 30-degree sector angle foil computed at 10k rpm	42
24	Maximum Foil Deflection of 30-degree sector angle foil computed at 10k rpm	42
25	Stress Distribution due to Pressure of 60-degree sector angle foil computed at 10k rpm	43



26	Maximum Foil Deflection of 60-degree sector angle foil computed at 10k rpm	43
27	Stress Distribution due to Pressure of 90-degree sector angle foil computed at 10k rpm	44
28	Maximum Foil Deflection of 90-degree sector angle foil computed at 10k rpm	44
29	Model of 90-degree sector angle foil with 0.1mm thickness	45
30	Model of 90-degree sector angle foil with 0.15mm thickness	45
31	Model of 90-degree sector angle foil with 0.2mm thickness	46
32	Model of 90-degree sector angle foil with 0.3mm thickness	46
33	Model of 90-degree sector angle foil with 0.4mm thickness	47
34	Model of 90-degree sector angle foil with 0.5mm thickness	47
35	Stress Distribution due to Pressure of 90-degree sector angle foil of 0.5mm thickness computed for 50k rpm	48
36	Maximum Foil Deflection of 90-degree sector angle foil of 0.5mm thickness computed for 50k rpm	48
37	Load on 90-degree sector angle foil computed for different foil thickness and speeds	49
38	Deflection of 90-degree sector angle foil computed for different foil thickness and speeds	50
39	2D drawing of 90-degree sector angle foil with viscoelastic support (Air bubble) in corner	51
40	Model of 90-degree sector angle foil with viscoelastic support (Air Bubble)	51
41	Stress Distribution due to Pressure of 90-degree sector angle foil with viscoelastic support (Air Bubble) computed at 30k rpm	52
42	Maximum Foil Deflection of 90-degree sector angle foil with viscoelastic support (Air Bubble) computed at 30k rpm	52
43	Sector angle 90-degree foil computed for viscoelastic support (Air Bubble)	53
44	Model of 90-degree sector angle foil with 2 viscoelastic support (Air Bubble) Case 1	54
45	Model of 90-degree sector angle foil with 2 viscoelastic support (Air Bubble) Case 2	54
46	Model of 90-degree sector angle foil with 2 viscoelastic support (Air Bubble) Case 3	55
47	Model of 90-degree sector angle foil with 3 viscoelastic support (Air Bubble) Case 4	55

## LIST OF TABLES

Table Number	Description	Page Number
1	Results of load obtained from 90-degree sector angle foil computed for Different thickness	49
2	Results of Deflection obtained from 90-degree sector angle foil computed for Different thickness	50
3	Results obtained from 90-degree sector angle foil computed for viscoelastic support (Air Bubble)	53
4	Best results obtained from all configuration	58

---

# **Chapter 1**

## **INTRODUCTION**

---

## 1. INTRODUCTION

The recent development in high-speed turbomachinery requires accurately designed gas bearings. To meet the demand of high-speed turbomachinery under different operating conditions, the accurate design of foil gas bearings and its behavior is a prerequisite for different applications. Viscous drag forces between the moving runner surface and the gas and the compliant spring-like structure of the bearing allow and form the film, which supports the bearing load.

This project mainly focuses on Airfoil Thrust bearing. These bearings can operate at very high-speed conditions, but the problem is that at low speed the lift is very less because only the pressure of the air has to lift the bearing when loaded axially. Historically the study of the theoretical performance of airfoil thrust bearing has been done but it also important to estimate the performance under actual operating conditions. It is also important to identify the parameters to be studied under actual operating conditions that affect the performance of AFTB.

A bearing is a machine element that allows constrained relative motion between two or more parts. Thrust bearings support the axial thrust of both horizontal as well as vertical shafts. Airfoil thrust bearings (AFTB) are self-acting, compliant surface hydrodynamic bearings which operate on a thin lubricating gas film. A converging gap in the direction of rotation compresses the gaseous lubricant to elevated pressure, separates the relatively moving surfaces, and provides a load-carrying capacity at elevated speeds. Viscous drag forces between the moving runner surface, gas, and the compliant spring-like structure of the bearing allow and form the film, which supports the bearing load. The performance of AFTB mainly depends on the design and construction of thrust runner and bearings and the selection of proper solid lubrication coatings. AFTB bearings are widespread use in oil-free microturbines and aircraft air cycle machines. The bearing consists of a solid backing plate with an annulus of discrete bearing pads or petals. Each of these pads is constructed from a smooth and continuous top foil that is fixed on the leading edge and free on the remaining edge. Once the thrust runner is spinning quickly enough, the working fluid [usually air] pushes the foil away from the runner so that there is no more contact. The runner and foil are separated by the air's high pressure which is generated by the rotation

---

which pulls gas into the bearing via viscosity effects. The high speed of the runner with respect to the foil is required to initiate the air gap, and once this has been achieved, no wear occurs. Unlike aero or hydrostatic bearings, foil bearings require no external pressurization system for the working fluid, so the hydrodynamic bearing is self-starting.

## 1.1 Journal Foil Bearing

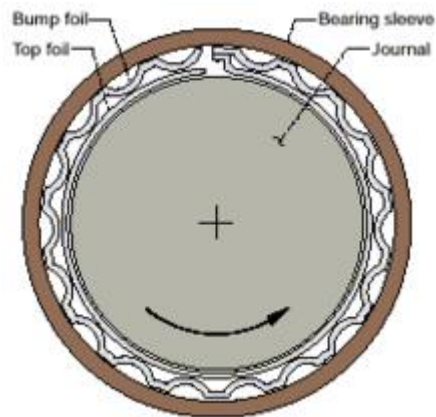


Figure 1 Journal Foil Bearing [20]

A Journal foil bearing is a type of air bearing. A shaft is supported by a compliant, spring-loaded foil journal lining. Once the shaft is spinning fast enough, the working fluid (usually air) pushes the foil away from the shaft so that no contact occurs. The shaft and foil are separated by the air high pressure, which is generated by the rotation that pulls gas into the bearing via viscosity effects. As high speed of the shaft with respect to the foil is required to initiate the air gap, and once this has been achieved, no wear occurs.

## 1.2 Working of Foil Bearing

Foil bearings typically operate without static clearance between the stationary foil and rotating shaft. There is often a preload between the bearing and runner parts. At a certain speed known as the lift-off speed, the hydrodynamic force overcomes the preload and complete fluid film lubrication is established. While the gas film prevents rubbing contact during normal operation, solid lubricants are applied to both foils and runners to prevent wear and galling during startup, shutdown, and overload conditions when sliding contact occurs.

---

## 1.3 Types of Airfoil Bearings

### Aerostatic Gas Bearings

- Aerostatic gas bearings are also known as externally pressurized gas bearings and an external pressurized air or gas is to maintain pressure between the bearing sleeve and the journal.
- Aerostatic bearings utilize a thin film of high-pressure air to support a load. Since air has a low viscosity, bearing's gap needs to be small, in the order 1-10  $\mu\text{m}$ .
- There are five basic types of aerostatic bearing geometries: single pad opposed pad, journal, rotary thrust, and conical journal or thrust bearings similar to hydrostatic bearings.

### Aerodynamic Gas Bearings

- Aerodynamic gas bearings are also known as self-acting bearings and an air film is created by the relative motion of two mating surfaces separated by a small distance. From rest, as the speed increases, a velocity induced pressure gradient is formed across the clearance.
- The increased pressure between the surfaces creates a load-carrying effect. The load capacity is dependent on the relative speed at which the surface moves and therefore at zero speed, the bearing supports no load. Zero loads at zero speed effect cause starting and stopping friction and results in some wearing of the bearing surfaces.

## 1.4 Applications of Airfoil Bearings

The first gas journal bearing was demonstrated by Kingsbury (1897). Gas- lubricated bearings are used in many industrial applications in which the hydrodynamic film of gaseous fluid is produced by hydrodynamic action. The gas is generally air. This avoids the need for a liquid lubrication system, simplifies the bearing design, and reduces maintenance. Gas bearings are used in gyroscopes where precision and constant torque are required, machine tool spindles, turbo-machinery, dental drills, food, and textile machinery and tape and disk drives as part of magnetic storage devices.

---

## 1.5 Thrust Bearing



Figure 2 Thrust Ball Bearing [21]

Thrust bearings are commonly used in automotive, marine, and aerospace applications. They are also used in the main and tail rotor blade grips of RC (radio-controlled) helicopters. Thrust bearings are used in cars because the forward gears in modern car gearboxes use helical gears which, while aiding in smoothness and noise reduction, cause axial forces that need to be dealt with. Thrust bearings are also used with radio antenna masts to reduce the load on an antenna rotator. One specific thrust bearing in an automobile is the clutch "throw out" bearing, sometimes called the clutch release bearing.

### 1.6 Thrust bearings come in several varieties.

- Thrust ball bearings, composed of bearing balls supported in a ring, can be used in low thrust applications where there is little axial load.
- Cylindrical thrust roller bearings consist of small cylindrical rollers arranged flat with their axes pointing to the axis of the bearing. They give very good carrying capacity and are cheap, but tend to wear due to the differences in radial speed and friction which is higher than with ball bearings.
- Tapered roller thrust bearings consist of small tapered rollers arranged so that their axes all converge at a point on the axis of the bearing. These are the type most commonly used

---

in automotive applications (to support the wheels of a motor car for example) they can support greater thrust loads than the ball type due to the larger contact area but are more expensive to manufacture.

- Spherical roller thrust bearings use asymmetrical rollers of spherical shape, rolling inside a house washer with a raceway with spherical inner shape. They can accommodate combined radial and axial loads and also accommodate misalignment of the shafts. They are often used together with radial spherical roller bearings. Spherical roller thrust bearings offer the highest load rating density of all thrust bearings.
- Fluid bearings, where the axial thrust is supported on a thin layer of pressurized liquid these give low drag.
- Magnetic bearings, where the axial thrust is supported on a magnetic field. This is used where very high speeds or very low drag is needed.

## **1.7 Fluid bearing**

Fluid bearings are bearings in which the load is supported by a thin layer of rapidly moving pressurized liquid or gas between the bearing surfaces. Since there is no contact between the moving parts, there is no sliding friction, allowing fluid bearings to have lower friction wear and vibration than many other types of bearings.

They can be broadly classified into two types: fluid dynamic bearings (also known as hydrodynamic bearings) and hydrostatic bearings. Hydrostatic bearings are externally pressurized fluid bearings, where the fluid is usually oil, water, or air, and the pressurization is done by a pump. Hydrodynamic bearings rely on the high speed of the journal (the part of the shaft resting on the fluid) to pressurize the fluid in a wedge between the faces. Fluid bearings are frequently used in high load, high speed, or high precision applications where ordinary ball bearings would have a short life or cause high noise and vibration. They are also used increasingly to reduce costs. For example, hard disk drive motor fluid bearings are both quieter and cheaper than the ball bearings they replace.



---

## 1.8 Hydrodynamic bearing

Hydrodynamic bearings work by floating the rotating components on a thin film of fluid and are often referred to as fluid film bearings. The separation of the rotating and stationary surfaces results in very low friction and negligible wear, giving the hydrodynamic bearing an exceptionally long life in many cases equivalent to the life of the machine.

## 1.9 Thrust Foil Bearing

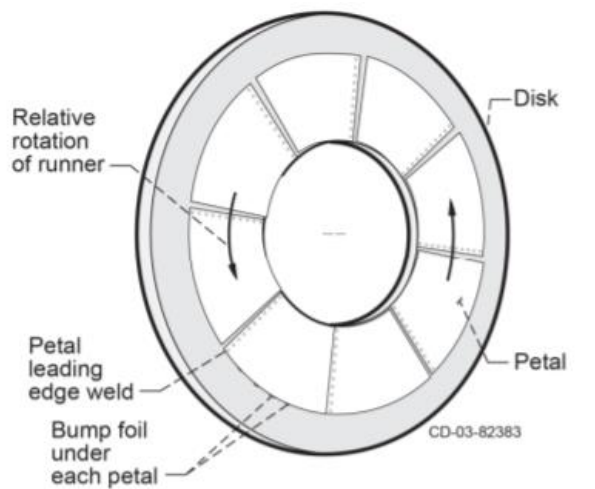


Figure 3 Thrust Foil Bearing [22]

A foil air bearing has a bump foil arranged on a thrust plate. A top foil includes a flat surface extending along with top bumps of the bump foil, an edge attached to the thrust plate, and a ramp connecting the edge and the flat surface. The ramp forms a curvature, the curvature has a center located in a field of classification search lower part of the ramp and tangentially contacts the top of a first bump of the bump foil. The foil thrust bearings are made up of three components. The backing plate which acts as a base for bearing. The bump foil act as a spring to absorb the load. The top foil provides a smooth surface for hydrodynamic air film generation. In hydrodynamic air foil bearing have an advantage that they do not need external air supply, but they require fabrication technology to fabricate bearing accurately.

## 1.10 Working of Thrust Foil Bearing

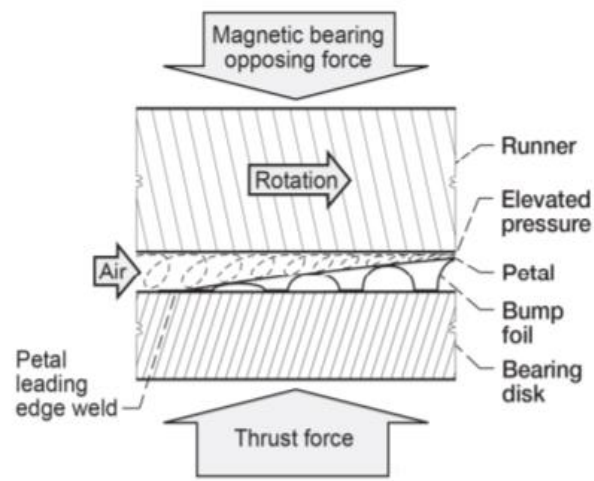


Figure 4 Thrust foil bearing principle of working [23]

In a thrust bearing, the converging film is developed between the foil and the runner due to the axial load. The hydrodynamic pressure rise is initially created by the physical contraction of the film thickness between the top foil and the thrust runner. The compliant foundation can take any number of styles and forms.

## 1.11 Pressure Development in Air Foil Thrust Bearing

The bearing consists of a solid backing plate with an annulus of discrete bearing pads or petals. Each of these pads is constructed from a smooth and continuous top foil that is fixed on the leading edge and free on the remaining edge.

Once the thrust runner is spinning quickly enough, the working fluid (usually air) pushes the foil away from the runner so that there is no more contact. The runner and foil are separated by the air's high pressure which is generated by the rotation which pulls gas into the bearing via viscosity effects. The high speed of the runner with respect to the foil is required to initiate the air gap and once this has been achieved no wear occurs.

---

The top foil provides a smooth flow for the gas film to develop onto generate hydrodynamic pressure. The airflow in the circumferential direction, as induced by the interaction with the air viscosity and the rotating surfaces, gets compressed into the groove.

## **1.12 History**

A recent development in high-speed turbomachinery requires accurately designed gas bearings. There are two types of gas bearings, journal foil bearing and foil thrust bearing. Foil gas journal bearing has been studied thoroughly than the foil gas thrust bearing. To understand the basic working principle and construction of airfoil thrust bearing (AFTB) there are open sources or handbooks on lubrication [24] available. To meet the demand of high-speed turbomachinery under different operating conditions the accurate design of foil gas bearing and its behavior prerequisites for different applications. Airfoil thrust bearing can operate at very high-speed condition, but the problem is at low speed the lift is very less because only the pressure of the air has to lift the bearing when loaded axially. So, there is a need for improvement in the design, ease of manufacture, and load-carrying capacity.

Historically the study of the theoretical performance of airfoil thrust bearing has been done but it is also important to estimate the performance under actual operating conditions. It is also important to identify the parameters to be studied under actual operating conditions which affect the performance. In the literature survey, an attempt has been made to identify performance influencing parameters by theoretical analysis and experimental methods on airfoil thrust bearings. The airfoil thrust bearings are made up of three components. The backing plate which acts as a base for bearing. The bump foil act as a spring to absorb the load. The top foil provides a smooth surface for hydrodynamic air film generation. In hydrodynamic air foil bearing have an advantage that they do not need external air supply, but they require fabrication technology to fabricate bearing accurately. To realize these needs of the airfoil thrust bearing, the design of bearing and fabrication of test rig for testing is very important. This section highlights the development taken in airfoil thrust bearing in the past decade.

The main requirement for testing of AFTB is the development of test rigs. The first low speed and high-speed test rig were developed by NASA which can be operated in a wide range of

---

operating conditions encountered in future oil-free gas turbines. S. Bauman [25] designed test rig to operate at very high speed and temperature conditions. Using this test rig the parameter like bearing torque, load, bearing lift-off/ touchdown speed, and temperature are measured. Using the conventional AFTB which was designed by NASA to conduct tests. These bearings are made up of series of segmented petals arranged circumferentially on a backing plate. The petals lie on bump foil. From the test, it was concluded that this tested data can be used for the future development of the analytical performance model.

### **1.13 Applications**

Turbomachinery is the most common application because foil bearings operate at high speed. The main advantage of foil bearings is the elimination of the oil systems required by traditional bearing designs.

### **1.14 Advantages**

- Higher efficiency, due to a lower heat loss to friction, instead of fluid friction.
- Increased reliability.
- Higher speed capability.
- Quieter operation.
- Wider operating temperature range (40–2,500 °K).
- High vibration and shock load capacity.
- No scheduled maintenance.
- No external support system.
- Truly oil-free where contamination is an issue.
- Capable of operating above the critical speed.

---

## 1.15 Disadvantages

- Lower capacity than roller or oil bearings.
- Wear during start-up and stopping.
- The high speed required for operation.
- Less load capacity than rolling or oil bearings.
- Wear during start-up and shut down.
- Thermal management issues.
- A difficulty in modeling complex interaction between film and foil bump's support (dry friction damping).

---

## **Chapter 2**

# **LITERATURE SURVEY**

---

## 2. LITERATURE SURVEY

A review has been made to identify performance influencing parameters on foil thrust bearings. The main importance given is, Review on the airfoil thrust bearing. The survey includes

[1] **Dr. Hooshang Heshmat**, this paper describes breakthroughs in foil thrust bearings achieving a thrust load capacity in excess of 570 kPa (83 psi), supersonic tip speed of 625 m/s (2050 ft/s) and temperature capability of 815 °C (1500 °F). Compliant foil bearings surpass many of the inherently show-stopping and debilitating features of rolling element bearings. Foil Bearings not only provide an environmentally-friendly, oil-free system of support, but are also well suited for high speed and extreme temperature applications such as gas turbines, compressors, turbochargers, cryogenic-turbopumps, turboexpanders, high-speed motors, and others. Modern foil bearings have demonstrated stable operational capabilities at super-critical speeds due to their tribodamping intrinsicity and ability to operate with any process fluid (gas or liquid). Recent developments have allowed increased operating temperatures, soaring to 815 °C and above, thus, providing a broader operating temperature range from deep cryogenic to extremely high temperatures.

[2] **Quan Zhou, YuHou, Chunzheng Chen**, this paper presents test results of a gas thrust bearing with viscoelastic support which is designed for high-speed turbo-machinery. The gas bearing, which belongs to compliant foil bearings, consists of a top thin metal foil and a bottom thin rubber foil. Static and stability experiments are conducted on a high-speed gas turbine test rig. The static results indicate that the structural stiffness of test bearing generally increases with the increase in axial load and the decrease in thickness of the bottom foil. In the rotation tests, the rotor runs stably with small vibration amplitude, which is dominant in the waterfall plot during the whole speed up the procedure. It shows that test bearing has preferable stability characteristics for high-speed gas turbines. Test results show that the thickness of the bottom foil affects the structural stiffness of test bearing significantly.

---

[3] **Dykas, B.D.** in this paper from NASA attempted to develop a test rig intended for parametric performance testing. They developed a prototype of AFTB and presented a detailed methodology of design, construction, and methods of manufacturing at a low cost. They have conducted several experiments to verify proper bearing operation at a speed range of 23000rpm.

[4] **Dykas, B.D. & Tellier, D.W** in this paper they designed a test rig to study the performance and durability of AFTB at high temperature. Testing has been done at high temperatures and a speed up to 21000rpm. The thrust runner is made of Inconel 718 and coated with PS300 series coating to withstand high temperature. They measured bearing torque and power loss to correlate with load capacity. They concluded that the study of wear mechanisms and bearing failure mode provides vital information for further improvement in design.

[5] **Park D.** attempted to study the theoretically static and dynamic characteristic of AFTB. Their study mainly consists of the determination of static characteristics using finite difference method [FDM] and bump foil characteristics by FEM. They obtained static and dynamic characteristics under tilting and non-tilting thrust pad of bearing. The foil bearing developed by Bruckner was validated using the modeling and simulating the foil thrust bearing by MiaasKowski.W. They have developed a numerical model of AFTB to calculate pressure distribution, wear, and temperature changes for different inclination angles of the outboard region and bearing disc plane during operation.

[6] **Dickman, J.R. & Prahl, J.M** investigated the factors influencing the performance of AFTB, he manufactured foil gas thrust bearing and tested from 0 to 40000 rpm against two PS400 coated. Considering the effect of stiffness on the load capacity, the main difference was observed that under low loads when not all of the bump foils are seated against top foil and fully engaged condition, because of the variation in damping. These systems of Airfoil Thrust Bearings are often proprietary and not fully described in the open literature, which makes it difficult to evaluate foil bearing designs relative to one another when different tribological systems are employed. Most of the development of AFTB has done by NASA and Mohawk Innovative Technology, Inc. [MiTi], USA. From the literature, it is evident that except NASA and MiTi



---

other researchers have made theoretical analysis, static test rigs, and the miniature model of AFTB starting from 2.8mm diameter of the airfoil thrust bearing.

**[7] Yong-Bok Lee, Tae Young Kim, Chang Ho Kim & Tae Ho Kim** in their a thrust test facility was successfully developed to determine the relationship between load capacity and the deflection of a bearing. To predict the air clearance, the deflection of the elastic foundation was used in the air film height equation. Combined Dirichlet and Neumann-type boundary conditions were used for static load performance predictions. To verify the theoretical model, tests were performed with three different thrust air foil bearings with outer radii of 45, 50, and 55 mm. The rotating speed ranged from 10,000 to 25,000 rpm. From the test results, the model using nonlinear stiffness was in better agreement with the experimental results than the model using linear stiffness and the Thrust bump foil bearings have high load capacity when the operating speed is high.

**[8] Franck Balducchi, Romain Gauthier** this paper deals with the experimental analysis of the torque and lift-off velocity of a foil thrust bearing. The geometric characteristics of the foil thrust bearing follow the design recently proposed by Dykas 2009, “Design, Fabrication, and Performance of Foil Gas Thrust Bearings for Micro turbomachinery Applications”. A dedicated test rig was developed and enables the measurement of the speed, torque, and temperatures under the foils. The measurements underlined the importance of managing heat transfer in a foil thrust bearing. Results are presented for mild static loads ranging from 5 to 60N and rotation speeds comprised between 20 and 35 krpm. The value of the start-up torque was validated by comparisons with results obtained with a rapid camera.

**[9] Tae Ho Kim, Tae Won Lee** their study aimed to develop a design guideline for increasing the load capacity of GFTBs. To predict the ultimate load capacity of the GFTB, the pressure was averaged in the radial direction of the gas flow field used to deflect the foil structure. The load capacity, film pressure profile, and film thickness profile were predicted for a GFTB with an outer radius of 55 mm, an inner radius of 30 mm, and eight foils each of arc length 45°. The predictions showed that the load capacity of the GFTB increased with increasing rotor speed and decreasing minimum film thickness and was always lower than the analytically determined limit

---

value for infinite rotor speed (obtained by simple algebraic equations). The predictions for a ramp height of 0.155 mm were in good agreement with the experimental data for all three test GFTBs with outer radii of 45, 50, and 55 mm, respectively. Also, this paper shows that the predicted drag torque increases linearly with increasing rotor speed and decreasing minimum film thickness, and nonlinearly with decreasing ramp height. The drag torque significantly increased only for ramp heights below the optimal value. The predictions imply that the optimal ramp height improves the load capacity of the GFTB with little change in the drag torque.

**[10] Luis San Andres, Keun Ryu, Paul Diemer** in this paper The prediction of the static and dynamic forced response of GFTBs, A laminar flow, thin-film flow model governs the generation of hydrodynamic pressure and a FE plate model determines the elastic deformation of a top foil and the under spring support, namely, bump strip layers. A perturbation analysis produces zeroth and first-order equations for prediction of the GTFB static load and drag torque, and the axial stiffness and damping force coefficients, respectively. The force coefficients are frequency-dependent due to the fluid compressibility, the flexibility of the top foil and the resilience of the bump strips support structure.

The experimental data are limited to load capacity and drag torque. Also, the model predicts, as an excitation frequency increases, a TFB axial stiffness that hardens and an axial damping coefficient that decreases rapidly. Predictions for a GTFB designed for use in an oil-free TC application account for the operating temperature range and increasing axial loads in the operating speed range. The GTFB friction factor is approximately constant,  $f_{0.009}$  to 0.015, over the whole speed range. The TFB stiffness and damping coefficients vary in their expected form as the excitation frequency increases. The operating gas temperature plays an insignificant role in the variation of the force coefficients with excitation frequency. On the other hand, the operating speed and the ensuing applied thrust load determine the largest change in the TFB force coefficients. As the known appropriate characterization of the mechanical energy dissipation in the sliding dry-friction between the bump foils and its foundation structure remains as a major unknown. Material or hysteretic damping is known to represent the best-measured results.

However, this parameter depends not only on the material properties and geometry but also on the operating conditions, including atmospheric conditions, as well as the current state of the

---

surfaces, inevitably degrading after extended periods of operation. Reliable loss factors are a must to ensure the adequate performance of GFTBs. Hence, the work toward developing a tool integrating both radial and thrust foil bearings for the design, prototyping, and troubleshooting of oil-free automotive turbochargers.

**[11] Kai Feng, Liang-Jun Liu, Zhi-Yang Guo, and Xue-Yuan Zhao** in this paper they theoretically analyzed the static and dynamic characteristics of GFTBs. First, the link-spring model introduced by Feng and Kaneko was used to simulate the characteristics of the bump foil. The top foil was described as an FE shell model to include deformation. Finally, these equations and the structural deflection equation were solved using the Newton–Raphson methods to account for the fluid-structure interaction. The predicted load values were compared with the published experimental data, and the results validate the theoretical analysis. Both the static load and frictional torque increase considerably at an appropriate small tilting angle. These analyses and results can help improve the understanding of GFTBs and provide designers with theoretical guidance for structure design and optimization.

**[12] Franck Balducchi, Mihai Arghir And Romain Gauthier** This paper deals with the experimental analysis of the dynamic characteristics of a foil thrust bearing (FTB) designed according to specifications given by NASA scientists in 2009. The dynamic characteristics of the bump foil structure were measured for static loads comprised between 30 N and 150 N while measurements for the FTB were performed at 35krpm for 30 N, 60 N, and 90 N. Excitation frequencies were comprised between 150 Hz and 750 Hz. Results showed that the dynamic stiffness of the FTB increases with excitation frequency while the equivalent damping decreases. Both stiffness and damping increase with the static load but are smaller at 35 krpm compared to 0 rpm.

**[13] Yueqing Zheng, Tianwei Lai** in their study they made multilayer protuberant foil thrust bearings with six pads the experimental results show that the variation of the structural stiffness mainly depends on the loading force and the configuration of the bearing. For a specific load, the structural stiffness of the bearing decreases with more layers of protuberant foil, while it increases with the thickness of protuberant foil. The tests show that the friction torque of the bearing mainly depends on the loading force than the rotational speed. The maximum load

---

capacity is 43.9N for 5th bearing made of a top foil with 0.05mm thickness and three layers of protuberant foils with 0.05mm thickness.

[14] **Gen Fu, Alexandrina Untaroiu**, in their study, a 3D CFD model for a parallel six pads thrust foil bearing is built using ANSYS-CFX software. The full Navier- Stokes equations are solved in the fluid domain. Taking into account the rotational periodicity, the computational model is simplified and only one pad of the thrust foil bearing is analyzed. To predict the thermal property, the total energy with viscous dissipation is used. Practical boundary conditions are used in the baseline CFD model. The results of the baseline modes are further compared with a modified Reynolds equation solution. Based on this model, the geometry of the thrust foil bearing is parameterized and analyzed using the design of experiments (DOE) methodology. In this paper, the selected geometry parameters of the foil structure include minimum film thickness, inlet film thickness, the ramp extent on the inner circle, the ramp extent on the outer circle, the arc extent of the pad, and the orientation of the leading edge. A factorial design technique is employed to sample the design space in DOE. The objectives in the sensitivity study are selected as load force and friction torque. An optimal foil geometry is derived based on the results of the DOE process by using a goal-driven optimization technique to maximize the load force and minimize the friction torque. The results show that the geometry of the foil structure is a key factor for foil bearing performance. The numerical approach proposed in this study is expected to be useful from the thrust foil bearing design perspective.

[15] **Tianwei Lai, Yu Guo, Wei Wang** Copper wire supported foil thrust bearing (CWFTB), which can be applied in high-speed turbo-expander, adopts an underlying flat foil as elastic supporting that interconnected with copper wires. In this paper, the finite element model of the thrust bearing is developed incorporating the fluid film and foil deflections. Fluid-structure interaction (FSI) is realized through the serial solution of the fluid Reynolds equation and the plate Kirchhoff equation. The pressure profile of the gas film and deflections of the top foil and bottom foil are obtained through iteration. Static bearing performance such as bearing load and friction torque of the bearing is evaluated concerning bearing configuration such as taper/land ratio, taper height, and copper wire arrangements. The finite element numerical results are validated with data from experiments.

---

[16] **P Samanta and MM Khonsari** in this paper they performed A parametric analysis to examine the role of limiting the load on different geometric parameters for the bearing. The limiting value of load-carrying capacity for a particular bearing can be effectively calculated using the limiting case solution method described in this paper. The limiting load for a particular bearing configuration was also obtained using an approximate solution method. The limiting load value is independent of the speed of the bearing. The limiting load for the bearing takes into account the effect of structural parameters and geometric profile parameters of the bearing. A high value of the ramp and compliance yield a large limiting load.

[17] **Travis A. Cable, Luis San Andres** This paper details the design and manufacturing of a novel Rayleigh-step metal mesh foil thrust bearing (MMFTB) as well as its testing on a dedicated rig. Metal mesh structures offer significant material structural damping and can be easily procured at a fraction of the cost of a typical bump-foil strip layer. The MMFTB consists of a solid carrier, several stacked annular copper mesh sheets (wire diameter 0.25, 0.3, and 0.41 mm), and a steel top foil (0.127mm thick) that makes six pads (ID 50.8 mm, OD 1/2 ID), each 45 deg in extent. As the bearing moved toward the rotating collar to begin applying thrust, the local high spots rubbed against the collar before a hydrodynamic wedge could form to separate the surfaces. Without a robust sacrificial coating, metal-to-metal contact quickly disfigured the contacting top foil pads, erasing the etched step, and leading to failure. In concept, and on paper, the mesh sheets and the top foil lay flat against the bearing carrier, giving a false sense of uniformity in the design process. In actuality, a designer must consider the manufactured states of the individual components and how they assemble. A redesign of the bearing intends to overcome the existing flaws (highlighted herein) by incorporating a thicker top foil that is well anchored (to better withstand the effects of windage), a robust sacrificial coating, and hydrodynamic wedge accomplished via a circumferential taper on each pad.

[18] **Nguyen T. LaTray and Daejong Kim** in this paper detailed features of a novel GFTB test rig and test results of 38mm GFTB. The developed test rig runs up to 190krpm and measures bearing load capacity, frictional torque, and temperature across bearing ID and OD. The test rig is suitable for testing GFTB with OD from 30 mm to 40 mm. The test facility successfully tests a 38mm GFTB to its predicted load capacity of 75N (110kPa). The high-speed test rig was

---

successfully up to 190krpm and load capacity and power loss of small GFTB were measured up to 155krpm with the load capacity of 75N. From the rotor dynamics analysis and measured axial vibration of the thrust runner, it was determined the large vibration at around 160krpm is due to the conical mode of the runner shaft.

**[19] Kan Qin, Peter A. Jacobs, Joshua A. Keep, Daijin Li, Ingo H. Jahn** in this paper, a computational framework for the fluid-structure thermal simulations of foil thrust bearings is presented. Individual solvers and their coupling strategies are detailed together with validation cases. A detailed description of the implemented foil bearing heat transfer models is provided. The numerical tool is used to conduct a comparative study between a foil thrust bearing of the same geometry operating with air and CO<sub>2</sub>. This comparison highlights several differences in bearing operation, in particular the heat fluxes and cooling requirements. Numerical simulations of foil thrust bearings with air and CO<sub>2</sub> are performed here. It is found that the high fluid density provides a new and effective cooling mechanism for the CO<sub>2</sub> bearing. Which is approximately 10 times more effective than air. Applying forced convection in the bump channels is an effective approach to enhance cooling, this will be essential for bearings operating at higher loads. High speeds can cause the temperature to dissipate, due to the weak conduction rate of the foil structure and also the low heat capacity air.

---

## **Chapter 3**

# **OUTCOMES OF LITERATURE SURVEY**

---

### 3. OUTCOMES OF LITERATURE SURVEY

From the literature survey, it is observed that at higher speeds the load-carrying capacity is less and deflection if foil is more, we got to know the problems and solutions obtained by the various researcher who researched this field the outcomes of this literature survey is listed below.

- With more layers of the protuberant foils and thinner top foil, the bearing shows a larger maximum load capacity.
- The variation of the structural stiffness mainly depends on the loading force and the configuration of the bearing.
- We got to know Thrust bump foil bearings have high load capacity when the operating speed is high.
- We found that structural stiffness of test bearing generally improves with the increase in axial load and decrease in thickness of bottom foil.

By the above point that we observed from various journals and research papers, we got an idea that what are all the problems and in which area the solution can be found out.



---

## **Chapter 4**

# **PROBLEM DEFINITION**

---

## 4. PROBLEM DEFINITION

From the literature survey, we found out various problems faced by the various researcher who researched this field which is listed below.

- The deformation of foil is found to be more due to friction.
- The dynamic stability of the airfoil bearing is low at higher speeds.
- The load-bearing capacity of high-speed bearing is less.
- The efficiency of conventional bearing is less

we are looking towards finding the solution for improvement in the performance of the thrust foil bearing by conducting various analysis and simulations and improvements in design and changing the design configurations trying to increase performance.

---

## **Chapter 5**

### **OBJECTIVES**

---

## 5. OBJECTIVES

This project aims to model and test an efficient thrust foil bearing for better performance over high speeds. The objectives of this project would be to:

- To improve the Load-carrying capability by varying the number of foils in bearing.
- To increase the efficiency by altering foil thickness and improve performance by proper designing of foil shape.
- To reduce the deformation of foil by supporting foil with viscoelastic material.

In our design, we are looking to minimize deflection of foils and increase the load-carrying capacity of the thrust foil bearing and to improve the performance of thrust foil bearing at higher speeds and we are looking to change foil shape and provide support to foil to increase the load-carrying capacity of a thrust foil bearing at higher speeds.

We aim to make a simulation model and test it analytical or by using software to find the maximum best possible results.

---

## **Chapter 6**

# **METHODOLOGY**

---

## 6. METHODOLOGY

To give a sound model of a thrust foil bearing a proper methodology has to be adopted:

- A suitable material for the foil and bearing block is selected.
- Designing of foil geometry and bearing block with appropriate dimensions using design software.
- Fabrication and assembling of foil and bearing block.
- Conducting Experiments on the fabricated model and record the results.
- Analysing the model through respective software and obtain the result values and comparing experimental and analytically obtained results.

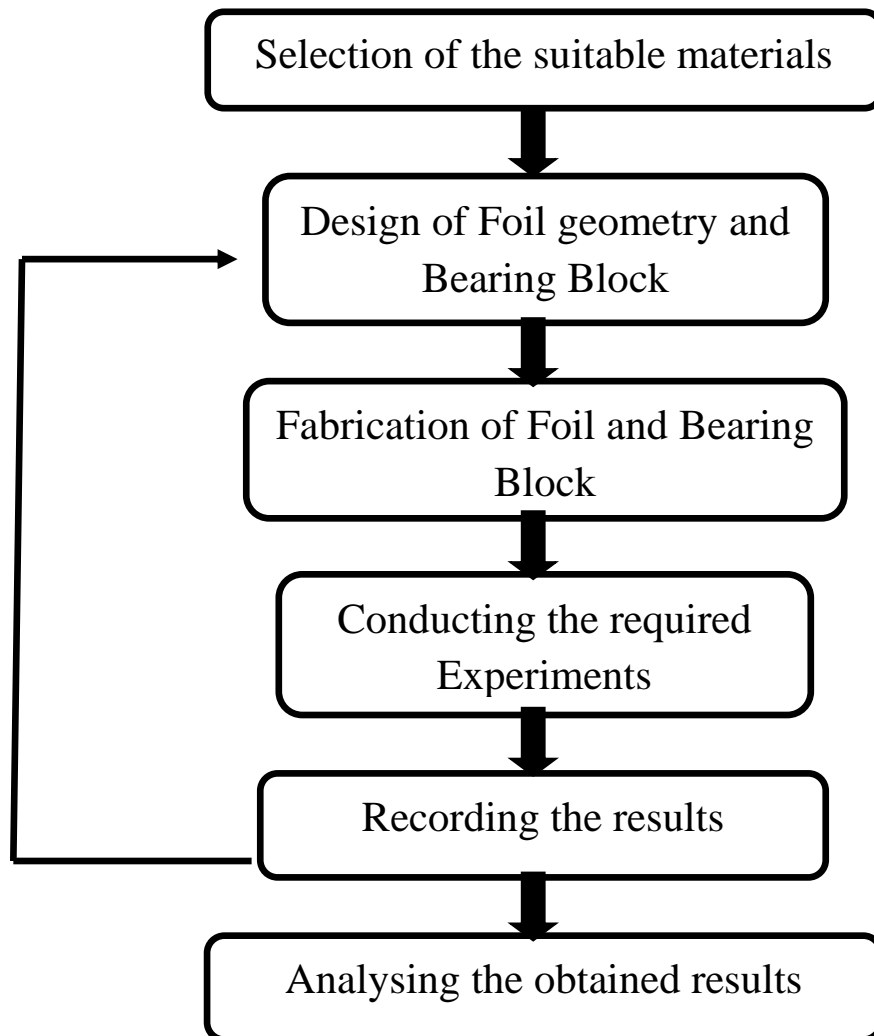


Figure 5 Methodology Flow Chart

---

## **Chapter 7**

# **DESIGN ASPECTS AND FABRICATION**

---

## 7. DESIGN ASPECTS AND FABRICATION

### 7.1 CAD Model of Thrust Runner

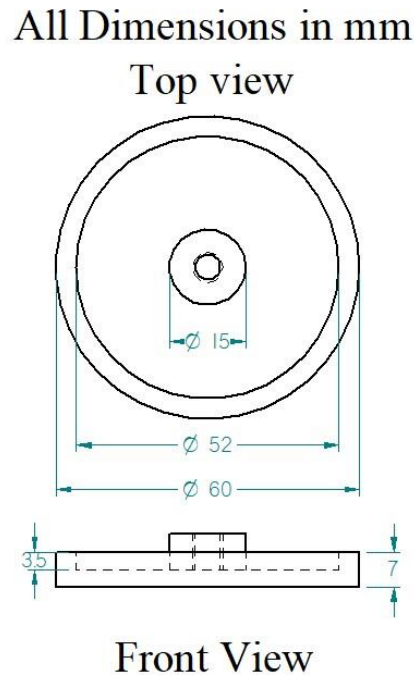


Figure 6 2D Model of Thrust Runner

Thrust runner is made of aluminum material and it provides a surface on which the air film is developed at higher speeds due to the hydrodynamic pressure. Initially, at the lower speed, the foil thrust bearing will be in contact with the runner and works as a conventional thrust bearing. The thrust runner should provide a wear-resistant surface at a lower speed and should have a good heat dissipating capacity.

### 7.2 CAD Model of Bearing block

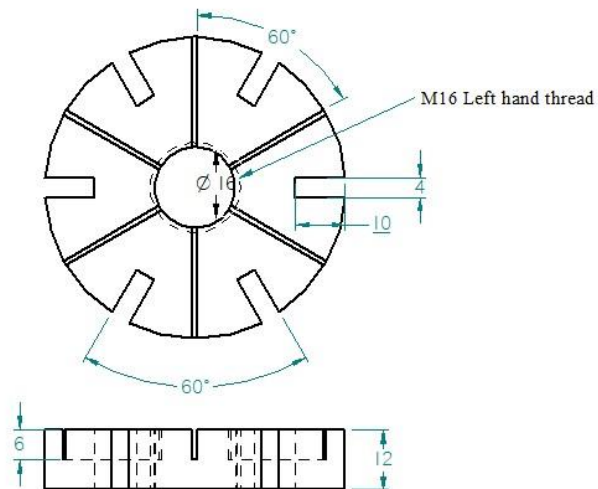
The bearing block is made up of aluminum material and the bearing block consists of six grooves to fix shim in the slots the figure below shows the design of the bearing block. Foil gas thrust bearing is self-acting, compliant-surface hydrodynamic bearings which operate on thin lubricating gas film. Foil bearing is mounted above the thrust runner and will be in contact with it at normal low-speed operation. Whereas at higher speed, it develops a thin gas film and runs



without metal to metal contact. The bearing should have sufficient load carrying and coefficient of friction.

All Dimensions in mm

Top View



Front View

Figure 7 2D Model of Bearing Block

### 7.3 Different Sector Angles of Foils

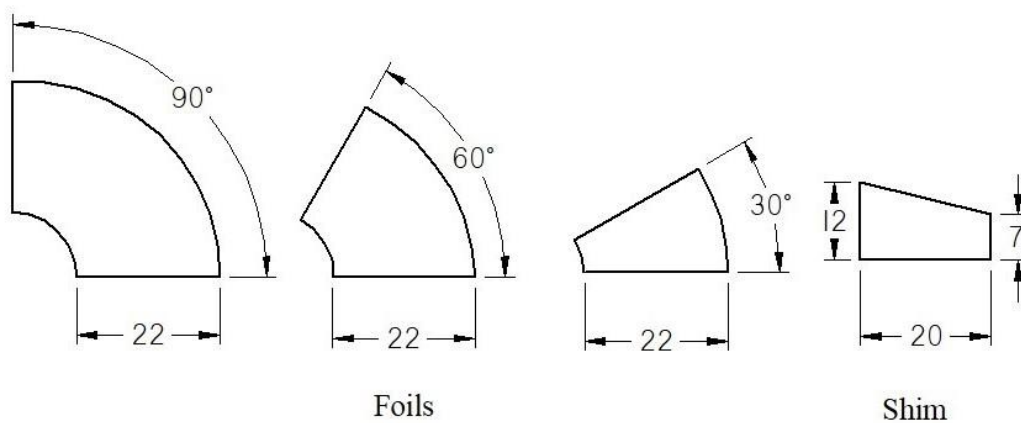


Figure 8 2D Model of 3 Different Sector Angle of Foils and a support Shim

---

When a circle is divided into four parts we obtain four 90 degree sector parts from the circle, then if we divide a circle into 6 parts we obtain six 60 degree sector parts and if we divide a circle into 12 parts we get twelve 30 degree parts this parts of a circle fit in the thrust foil bearing block as shown in models of thrust foil bearing. The divided parts of a circle are known as a sector angle.

#### **7.4 3D CAD Model of the Bearing block and Runner**

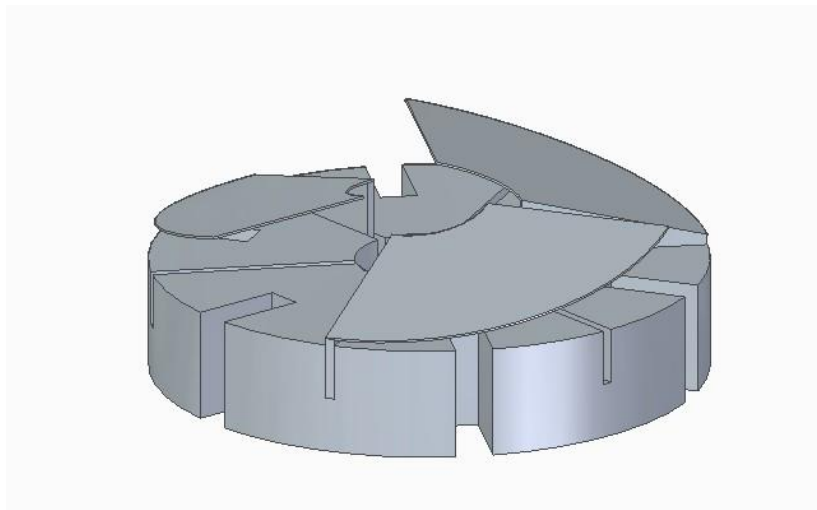


Figure 9 3D CAD Model and Assembly of Foils to Bearing Block

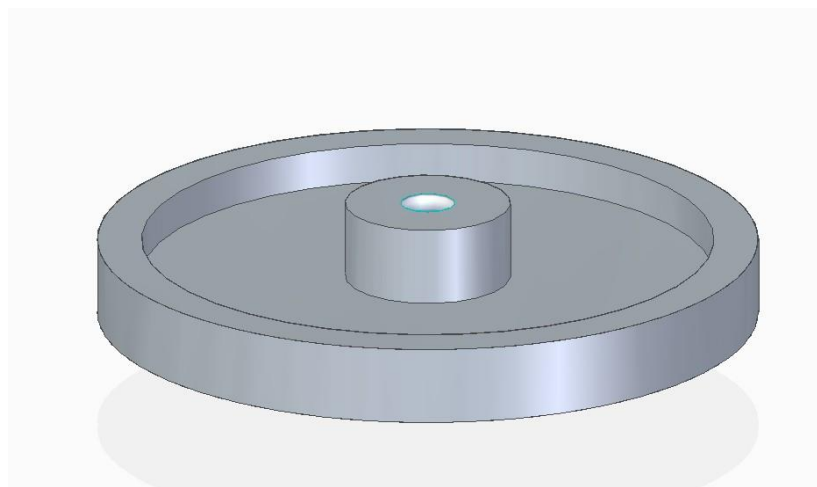


Figure 10 3D CAD Model of Runner

## 7.5 Runner and Bearing block with foil assembly

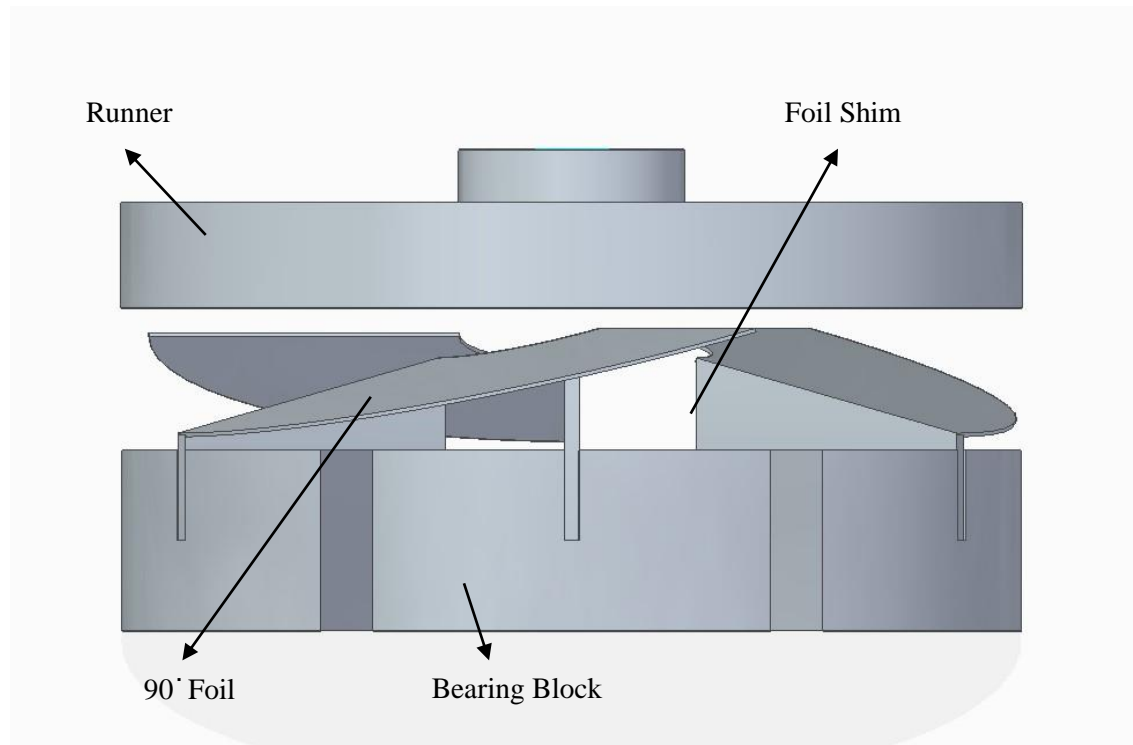


Figure 11 3D CAD Model Assembly of Bearing Block, Runner and 90 Degree Sector angle Foils

The above figure shows the assembly of thrust runner and bearing block with support shim and 90-degree sector angle foils attached to the bearing block and this is how a typical test model of a thrust foil bearing looks

## 7.6 Fabrication

- Raw material selection (aluminum).
- Turning, threading cutting, groove cutting as shown in 2D CAD models.
- Cutting sheet metal (copper) in foils shape by hand or using a laser cutting machine.
- Fixing shim and foils to bearing block using glue or metal adhesives.

---

## **Chapter 8**

# **FLUID STRUCTURE INTERACTION SIMULATION**

## 8. FLUID STRUCTURE INTERACTION ANALYSIS USING COMSOL SOFTWARE

### FSI Simulation in COMSOL 5.0v software

1. We downloaded the student version of COMSOL 5.0v from the [comsol.co.in](http://comsol.co.in) website and we learned how to use the software by the tutorials provided from them. COMSOL Multiphysics is a cross-platform finite element analysis, solver, and Multiphysics simulation software.
2. The expressions and equations can be entered in the parameter table given in the software. The parameter and equations that we used for the simulations are shown in the figure below in the table form.

Name	Expression	Unit	Description
r	$\sqrt{z^2+y^2}$	m	radial co ordinate xy plane
omega	$((2*3.142*10000)/60)[\text{rad/s}]$	rad/s	angular velocity
phi	$\text{atan2}(z,y)$	rad	azumithal angle
u	0		x component of moving...
v	$-\text{omega}*r*\sin(\phi)$	m/s	y component of vel
w	$-\text{omega}*r*\cos(\phi)$	m/s	z component of vel

Figure 12 Parameters and equations Table

3. The geometry that you see in the figure below is the boundary wall with foil inside, which is also called an air duct where airflow can be set to the required velocity.

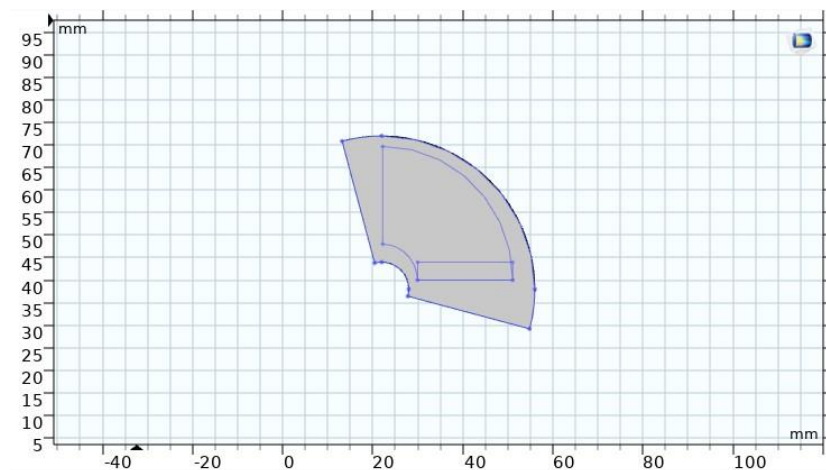


Figure 13 Air Duct (Boundary Wall) geometry

4. The geometry that you see in the figure below is the Shim Support which supports the foil the dimension is the same as seen in the design.



Figure 14 Shim geometry

5. The geometry that you see in the figure below is the 90-degree sector angle foil created and placed inside the air duct with the help of shim support.

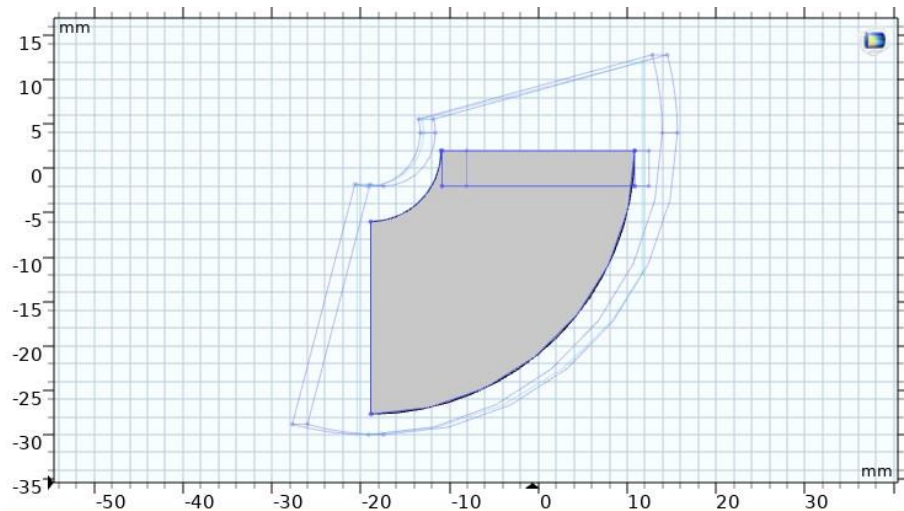


Figure 15 Foil Sector angle geometry

6. After creating the model the material should be selected the air duct is selected as a fluid that is air and Foil as Copper and the properties of the material selected should be specified in the table that is Young's modulus, Density, Dynamic viscosity, and Poisson's ratio of the material that you selected.



9. After meshing the model the computation should be done and wait for the simulation to complete then the results will appear on the model. The required 3d plots can be selected and plotted that are stress distribution, pressure distribution, and deformation as shown in the figure below.

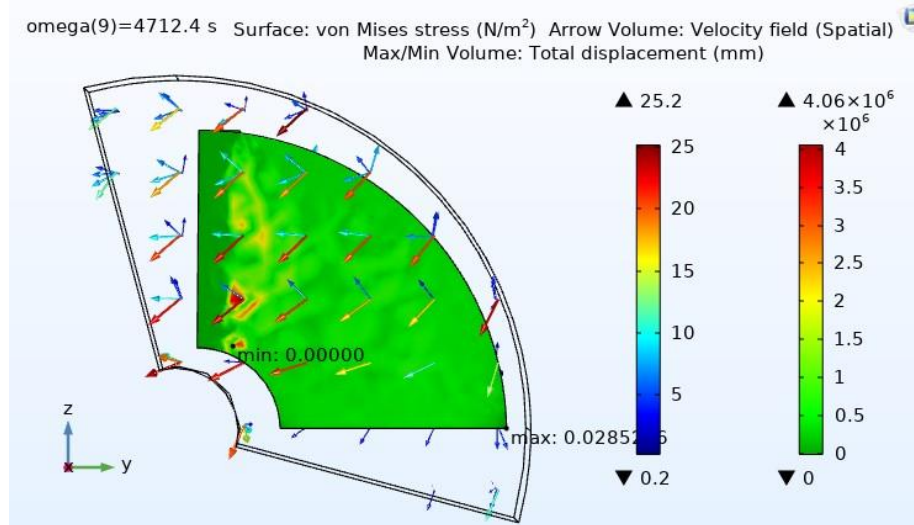


Figure 18 Stress Distribution and Air Flow

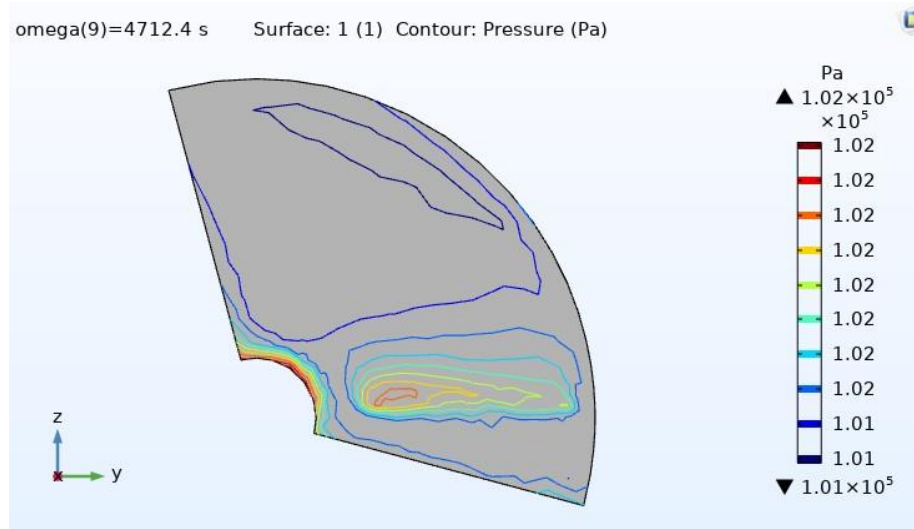


Figure 19 Pressure Contour

10. Foil surface and runner surface can be selected to plot stress contour on the foil surface and runner surface. The stress contour and pressure contour is shown in the figure above.



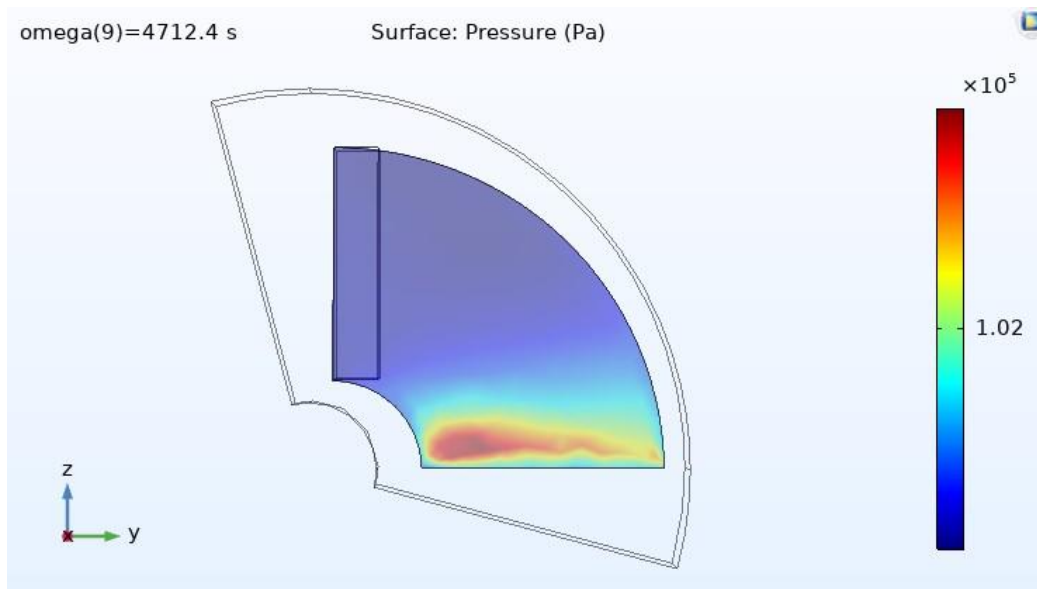


Figure 20 Stress Distribution due to Pressure on 90-degree foil surface

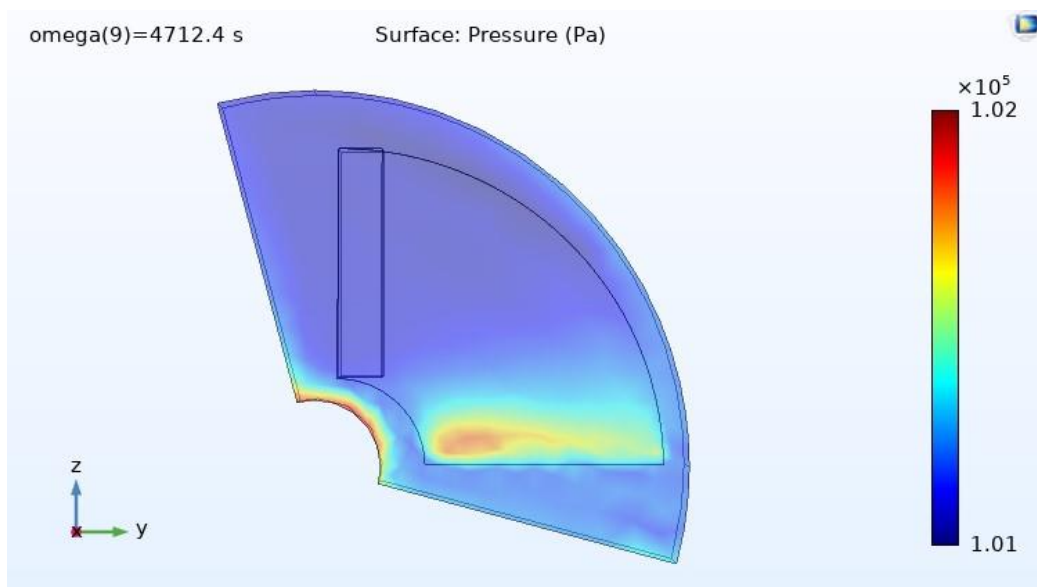


Figure 21 Stress Distribution due to Pressure on Runner surface

11. The stress distribution due to pressure can be plotted as show in the above figure, the stress concentration is high near the end of foil that is the red region see in the figure is the stress concentration at the tip of 90-degree sector angle foil. Also, we can plot the stress distribution on runner surface as shown in the figure above.

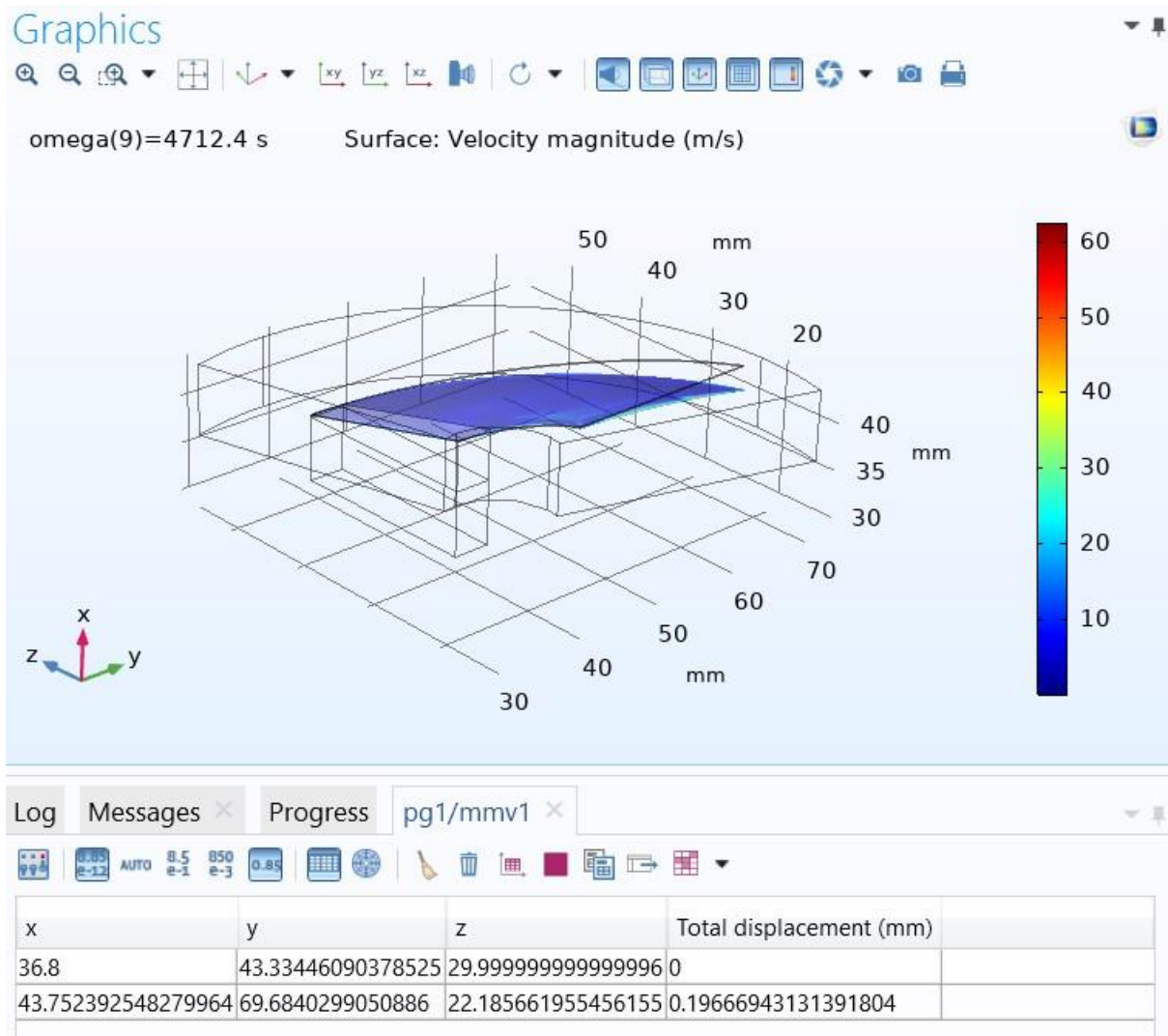


Figure 22 Displacement / Deflection of 90-degree sector angle foil

12. The deflection of the foil is calculated by the software and it is plotted in the form of a table as shown in the figure above.
13. In the software we can select surface and surface integration will be done by software and the results of Omega values and pressure values will be plotted as a table.
14. The table contains load in Newton for different Omega values obtained at different points on the foil surface and we can use the values to plots the line graph.

---

## **Chapter 9**

# **FSI SIMULATION RESULTS**

## 9. FSI SIMULATION RESULTS

### 9.1 Different Sector Angle Configurations

First, we modeled 30-degree sector angle foil and simulated for fluid-structure interaction in COMSOL 5.0v software the results are shown below.

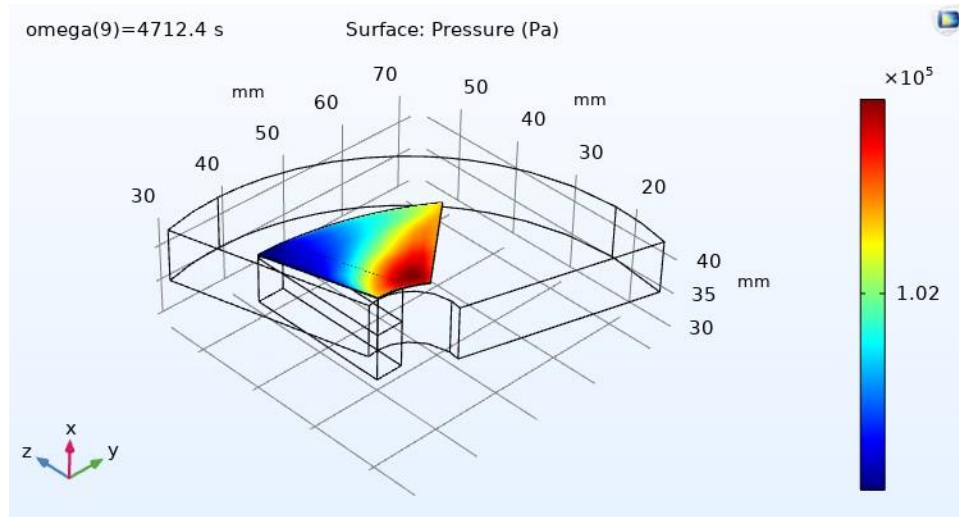


Figure 23 Stress Distribution due to Pressure of 30-degree sector angle foil computed at 10k rpm

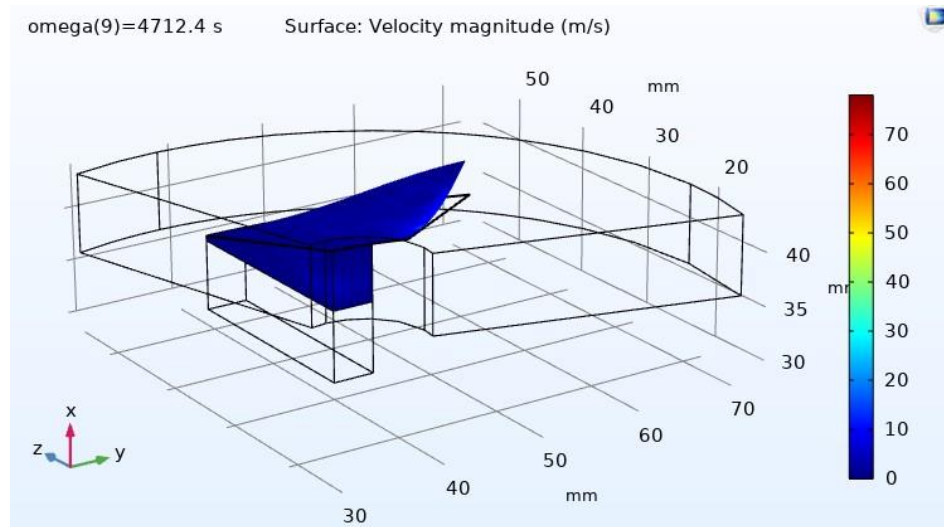


Figure 24 Maximum Foil Deflection of 30-degree sector angle foil computed at 10k rpm

The maximum load on foil at 10k rpm is around 34.7595 N and the Deflection is 0.0065 mm.

Then we modeled 60-degree sector angle foil and simulated for fluid-structure interaction in software the results are shown below.

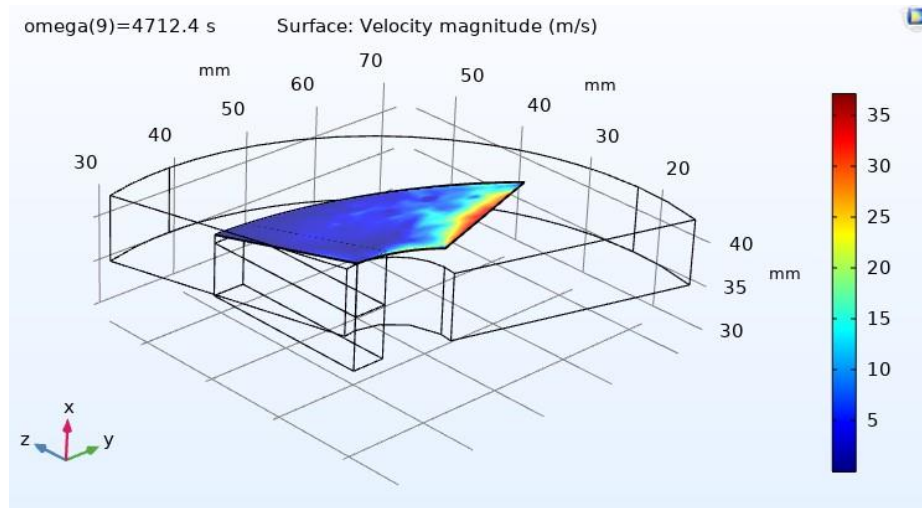


Figure 25 Stress Distribution due to Pressure of 60-degree sector angle foil computed at 10k rpm

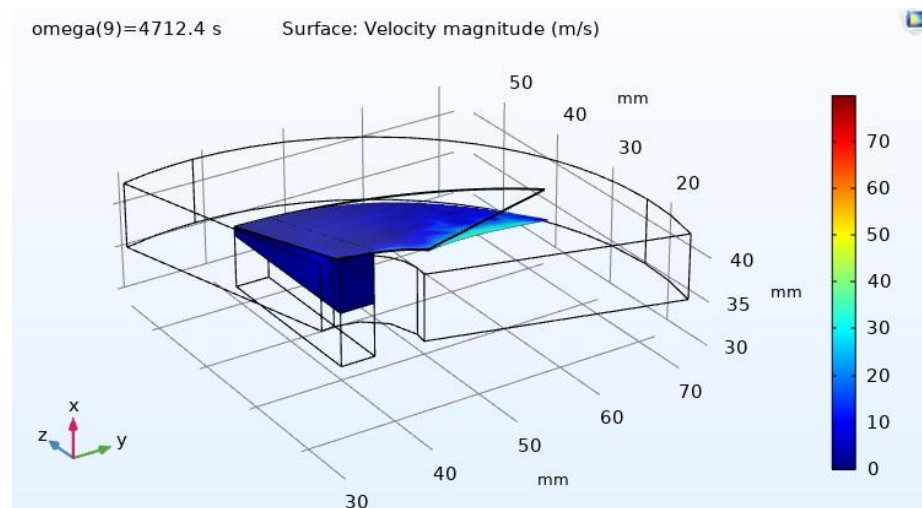


Figure 26 Maximum Foil Deflection of 60-degree sector angle foil computed at 10k rpm

The maximum load on foil at 10k rpm is around 48.61 N and the Deflection is 0.2179 mm. Here we can observe an improvement in load carrying capacity, so we decided to make a model of 90-degree sector angle foil and simulated for fluid-structure interaction in software the results are shown below.

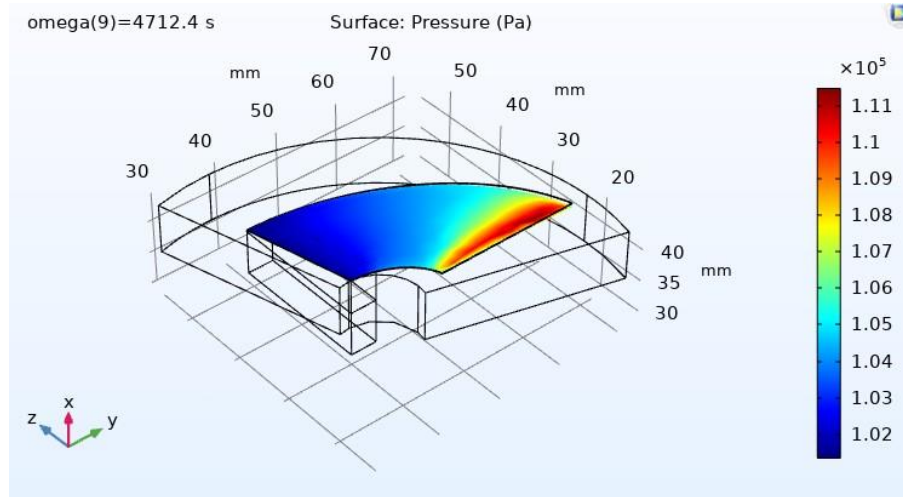


Figure 27 Stress Distribution due to Pressure of 90-degree sector angle foil computed at 10k rpm

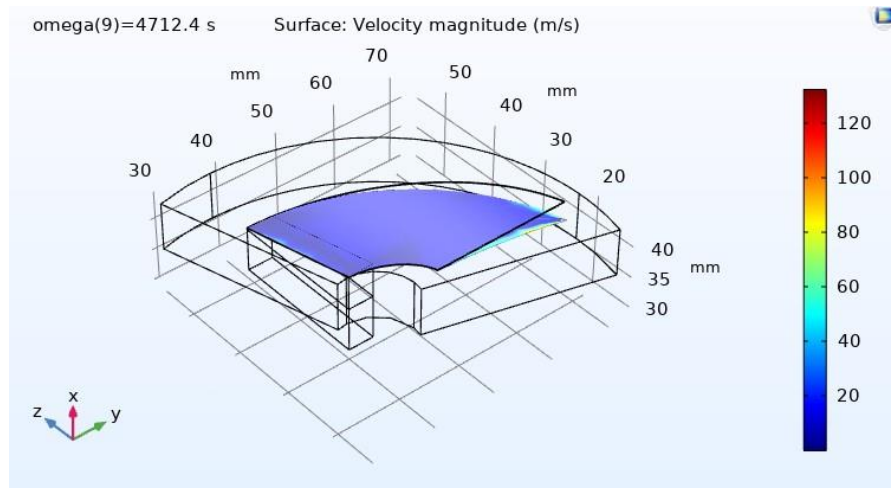


Figure 28 Maximum Foil Deflection of 90-degree sector angle foil computed at 10k rpm

We found that the maximum load on foil at 10k rpm is around 65.2041 N and the Deflection is 0.0285mm. Here in 90-degree sector angle foil, we can see an increase in load-carrying capacity when compared to a 30-degree sector angle and 60-degree sector angle.

## 9.2 Different Foil Thickness Configurations

After changing the sector angle configuration and Simulating we found out a 90-degree sector angle gives maximum load and less deflection when compared with another sector angles Configuration. So now we change the model by increasing the thickness of foil from 0.1mm,0.15mm,0.2mm,0.3mm,0.4mm, and 0.5mm the simulation results are shown below.

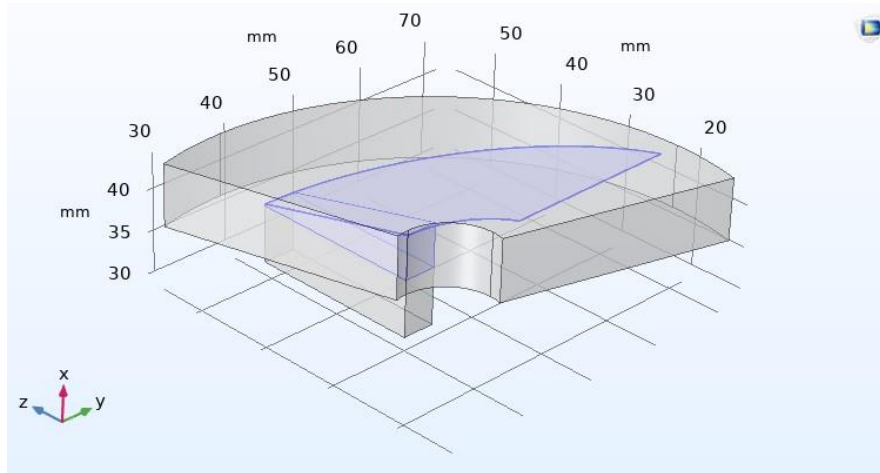


Figure 29 Model of 90-degree sector angle foil with 0.1mm thickness

We found that the maximum load on foil at 50k rpm is around 67.1952N and the Deflection is 0.5301mm in 90-degree sector angle foil with 0.1mm thickness Configuration. Then we again changed the thickness of foil to 0.15mm.

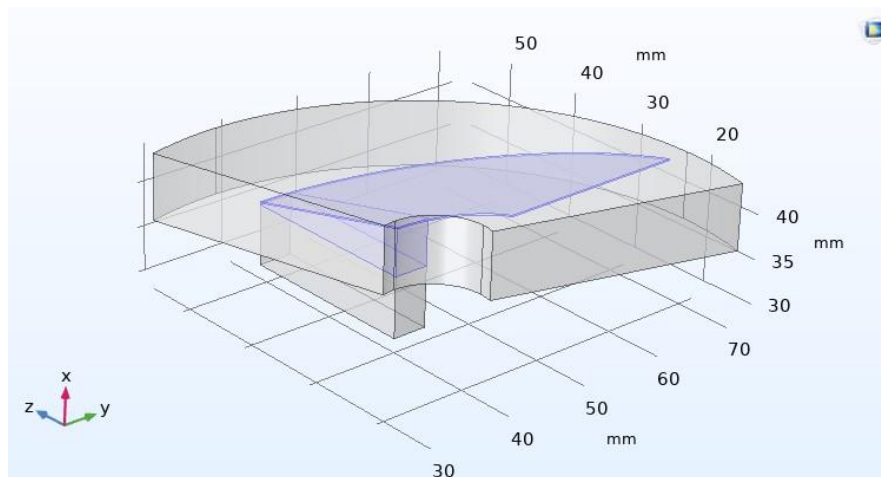


Figure 30 Model of 90-degree sector angle foil with 0.15mm thickness



We found that the maximum load on foil at 50k rpm is around 67.2754N and the Deflection is 0.7068mm in 90-degree sector angle foil with 0.15mm thickness Configuration. Here we can observe a little bit increase in load-carrying capacity and an increase in the deflection. We then again changed the thickness of foil to 0.2mm

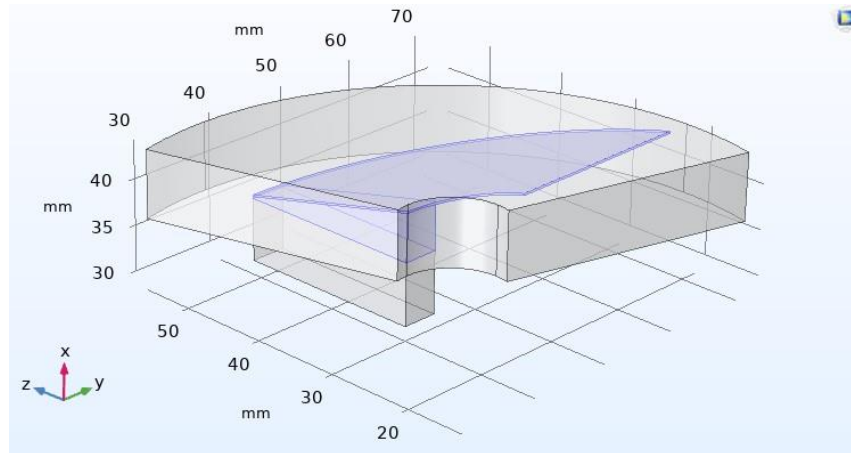


Figure 31 Model of 90-degree sector angle foil with 0.2mm thickness

We found that the maximum load on foil at 50k rpm is around 67.4255N and the Deflection is 0.5152mm in 90-degree sector angle foil with 0.2mm thickness configuration. Here we can observe a little bit increase in load-carrying capacity and a decrease in deflection. We then again changed the thickness of foil to 0.3mm

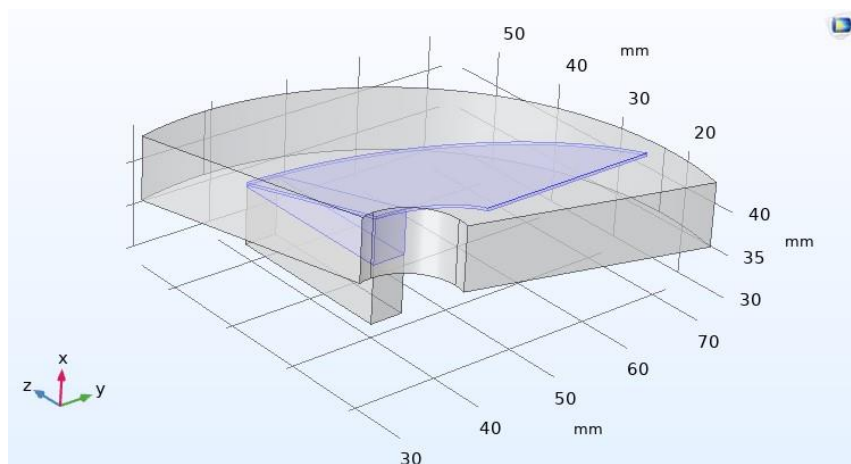


Figure 32 Model of 90-degree sector angle foil with 0.3mm thickness



We found that the maximum load on foil at 50k rpm is around 67.5790N and the Deflection is 0.4475mm in 90-degree sector angle foil with 0.3mm thickness configuration. Here we can observe a little bit increase in load-carrying capacity and a decrease in deflection. We then again changed the thickness of foil to 0.4mm

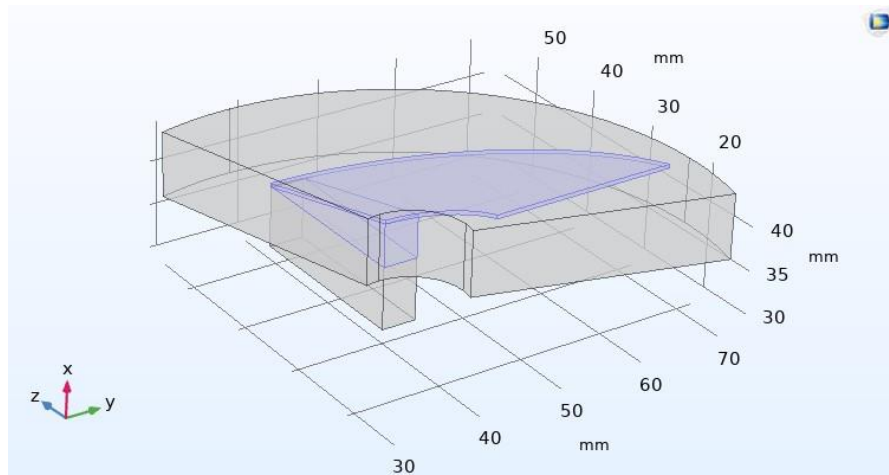


Figure 33 Model of 90-degree sector angle foil with 0.4mm thickness

We found that the maximum load on foil at 50k rpm is around 68.5936N and the Deflection is 0.4215mm in 90-degree sector angle foil with 0.4mm thickness configuration. Here we can observe a little bit increase in load-carrying capacity and a decrease in deflection. We then again changed the thickness of foil to 0.5mm

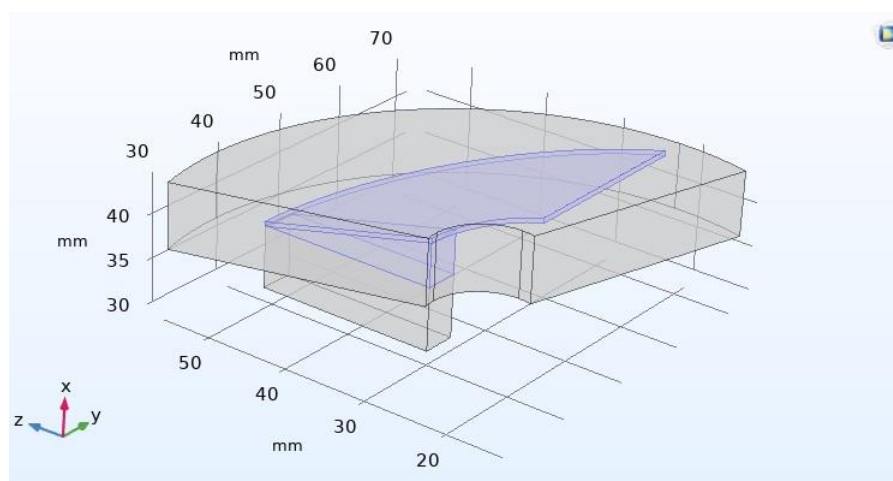


Figure 34 Model of 90-degree sector angle foil with 0.5mm thickness

We found that the maximum load on foil at 50k rpm is around 67.8318N and the Deflection is 0.1594mm in 90-degree sector angle foil with 0.5mm thickness configuration. Here we can observe a little bit decrease in load-carrying capacity and a decrease in the deflection.

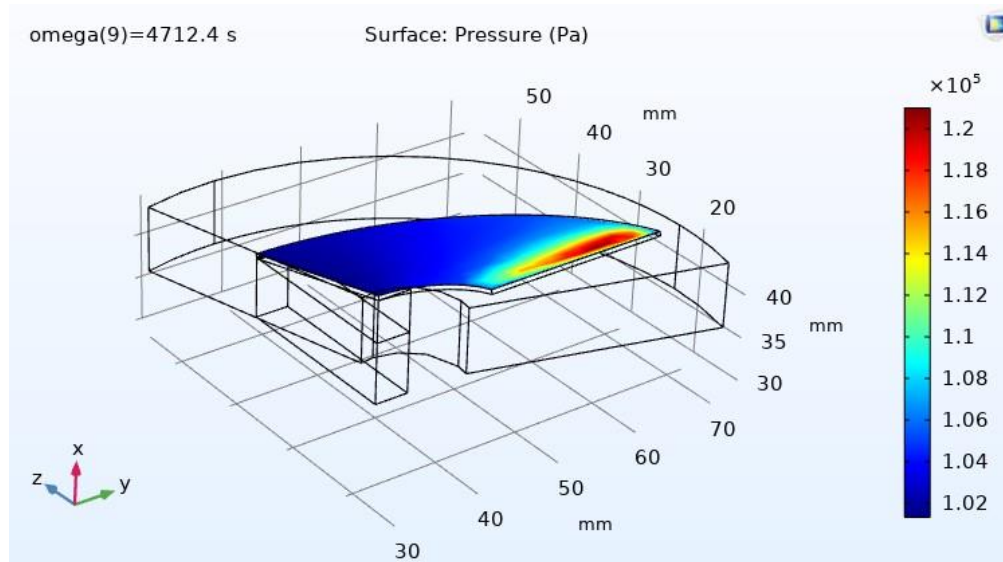


Figure 35 Stress Distribution due to Pressure of 90-degree sector angle foil of 0.5mm thickness computed for 50k rpm

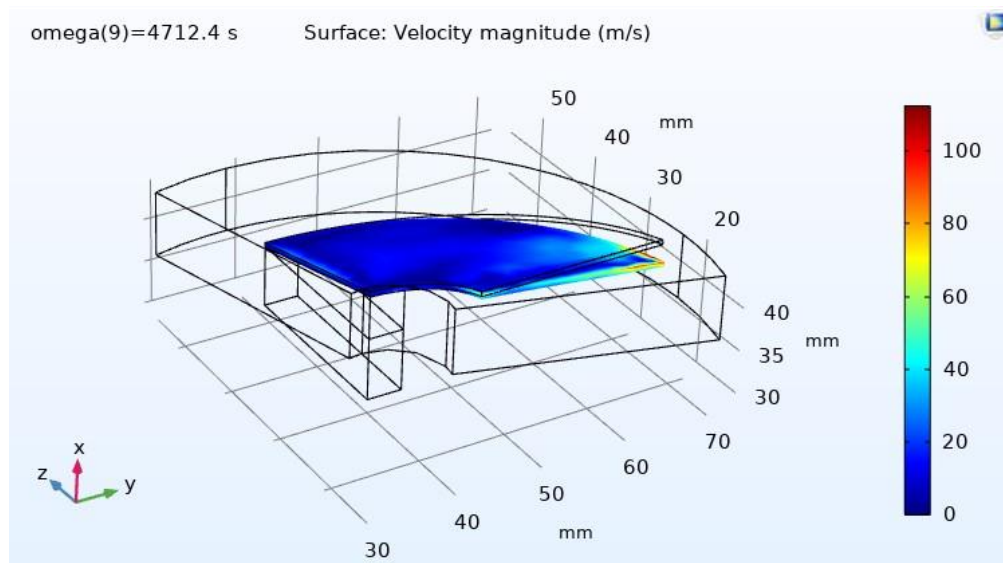


Figure 36 Maximum Foil Deflection of 90-degree sector angle foil of 0.5mm thickness computed for 50k rpm

Table 1 Results of load obtained from 90-degree sector angle foil computed for Different thickness

Speed in rpm	0.1mm foil Thickness	0.15mm foil Thickness	0.2mm foil Thickness
10000	65.20413842	65.20324287	65.21056239
20000	65.46856773	65.49296659	65.51702933
30000	65.88115381	65.94337681	66.00111518
40000	66.4816193	66.5392155	66.6412123
50000	67.19529135	67.19529135	67.42554269

Speed in rpm	0.3mm foil Thickness	0.4mm foil Thickness	0.5mm foil Thickness
10000	65.21919956	65.2109087	65.21211907
20000	65.55074524	65.55023533	65.5445701
30000	66.07140848	66.11789895	66.10043673
40000	66.75072603	66.90173975	66.86911703
50000	67.19529135	68.5936719	67.19529135

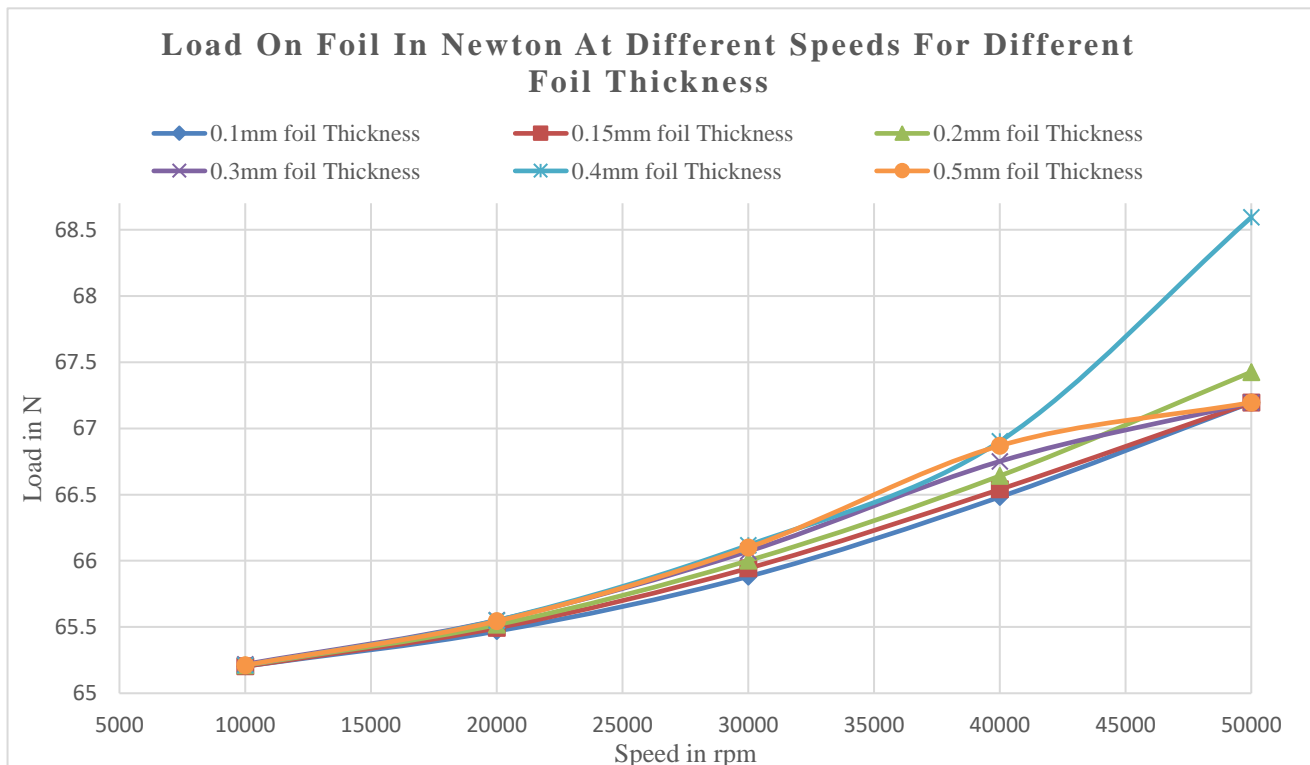


Figure 37 Load on 90-degree sector angle foil computed for different foil thickness and speeds

Table 2 Results of Deflection obtained from 90-degree sector angle foil computed for Different thickness

Speed in rpm	0.1mm foil Thickness	0.15mm foil Thickness	0.2mm foil Thickness
10000	0.028527628	0.059684884	0.036871419
20000	0.102739661	0.210738871	0.135097956
30000	0.196669431	0.394311532	0.266219992
40000	0.420391826	0.564327106	0.398767372
50000	0.530171896	0.706806672	0.515299299
Speed in rpm	0.3mm foil Thickness	0.4mm foil Thickness	0.5mm foil Thickness
10000	0.028774646	0.008813133	0.006976128
20000	0.108961404	0.03734459	0.02875054
30000	0.219726603	0.083289502	0.063873619
40000	0.336679538	0.140695564	0.10882198
50000	0.447518814	0.421516085	0.159463088

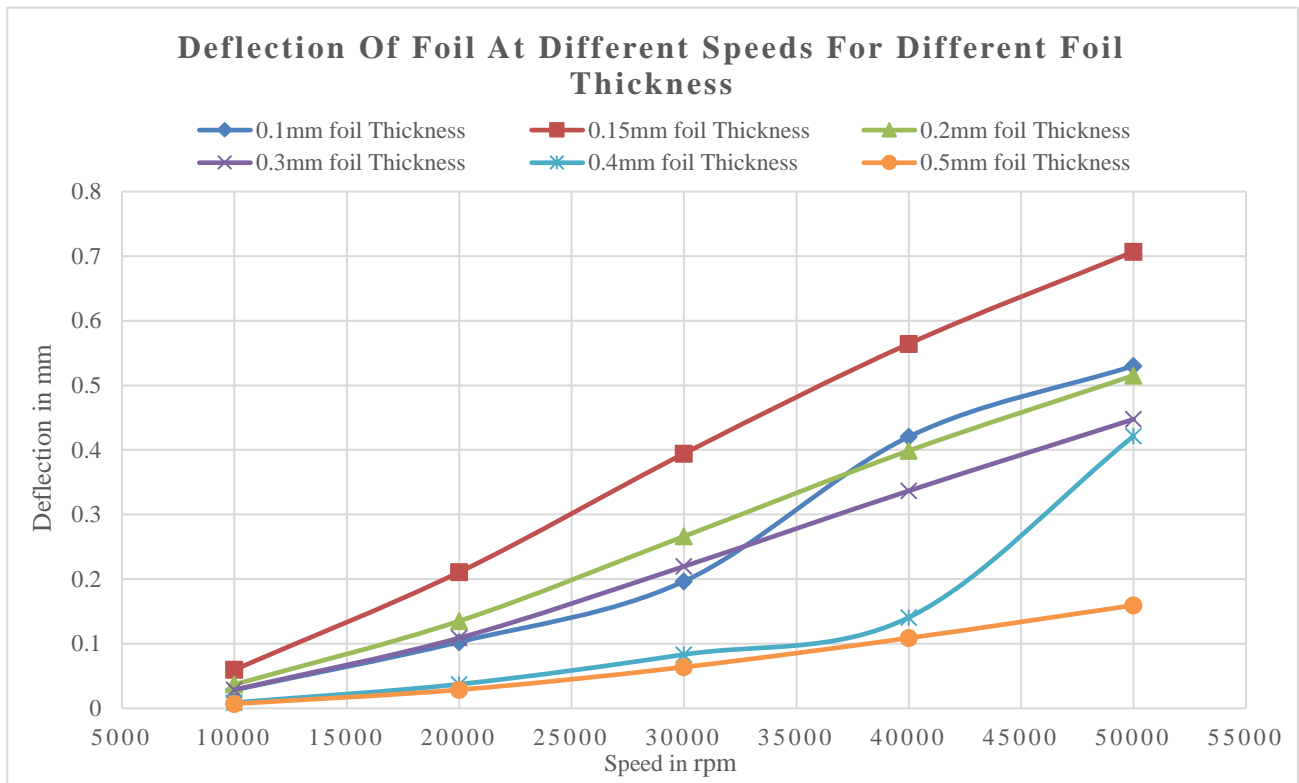


Figure 38 Deflection of 90-degree sector angle foil computed for different foil thickness and speeds

### 9.3 Viscoelastic Support Configuration

After changing the thickness, we found that increase in thickness decreases the deflection of foil and the foil deforms less when the thickness is more and little bit improvement in load-carrying capacity. So now we change the model by providing viscoelastic Support which u can see below. we modeled viscoelastic support for the 90-degree sector angle single foil with Viscoelastic support (Single Air Bubble from bubble wrap) in the corner of the foil and we gave the properties of the air bubble in software.

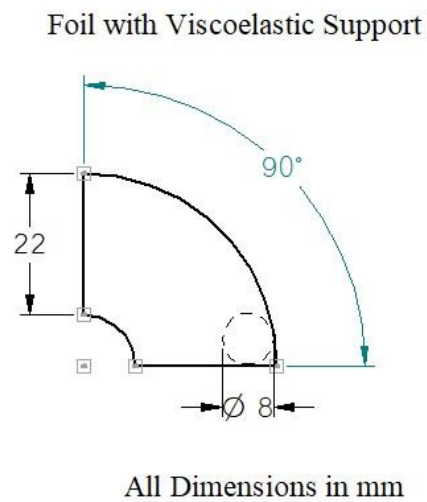


Figure 39 2D drawing of 90-degree sector angle foil with viscoelastic support (Air bubble) in corner

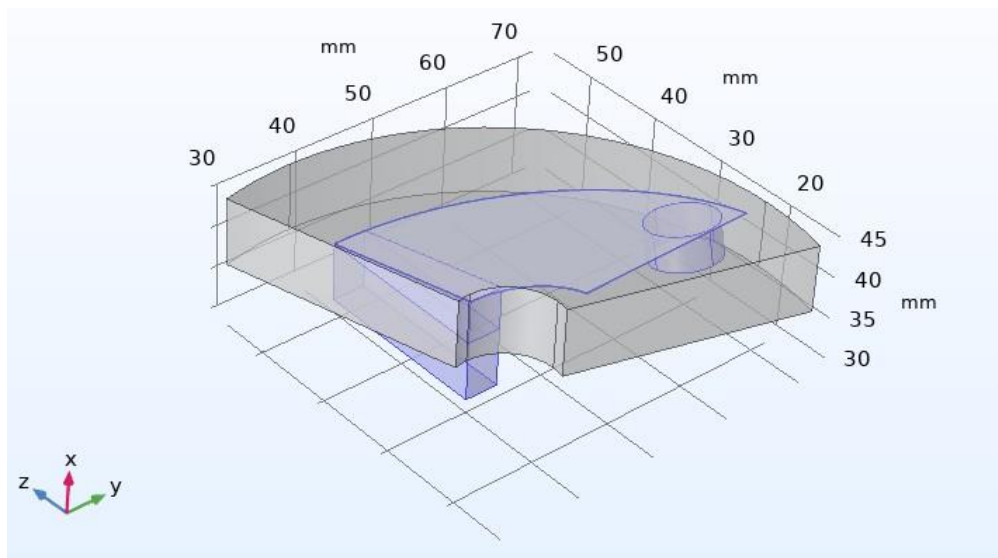


Figure 40 Model of 90-degree sector angle foil with viscoelastic support (Air Bubble)

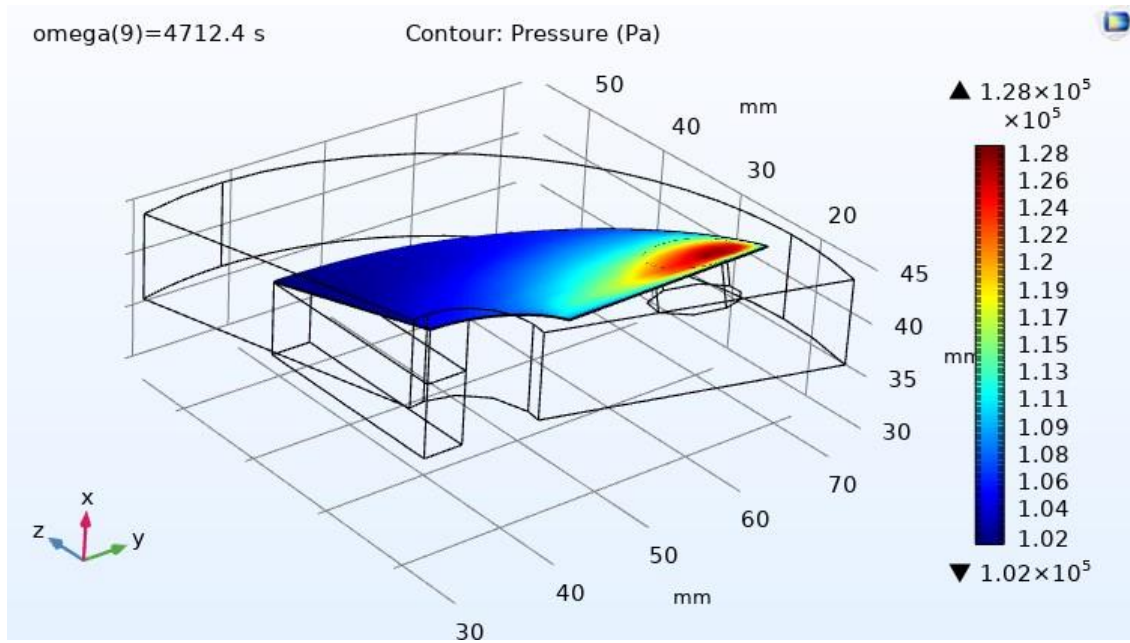


Figure 41 Stress Distribution due to Pressure of 90-degree sector angle foil with viscoelastic support (Air Bubble) computed at 30k rpm

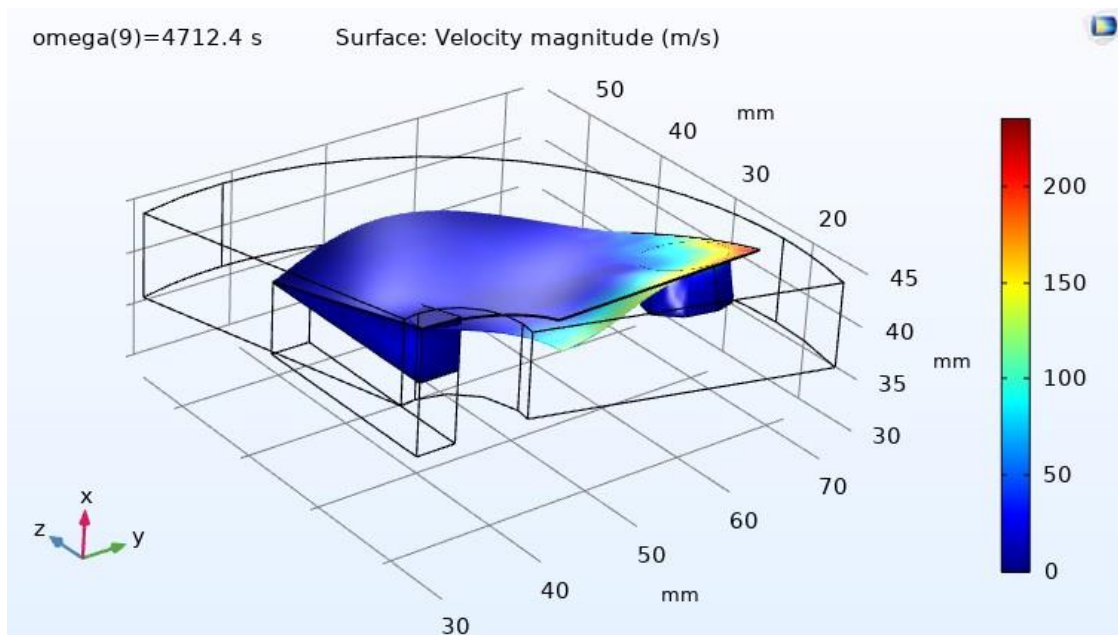


Figure 42 Maximum Foil Deflection of 90-degree sector angle foil with viscoelastic support (Air Bubble) computed at 30k rpm

Table 3 Results obtained from 90-degree sector angle foil computed for viscoelastic support (Air Bubble)

Speed in rpm	Load in N	Deflection in mm
10000	65.54880562	0.018670874
15000	66.2015411	0.040576792
20000	67.12083585	0.068968596
25000	68.3006367	0.100636894
30000	69.74827118	0.133838942

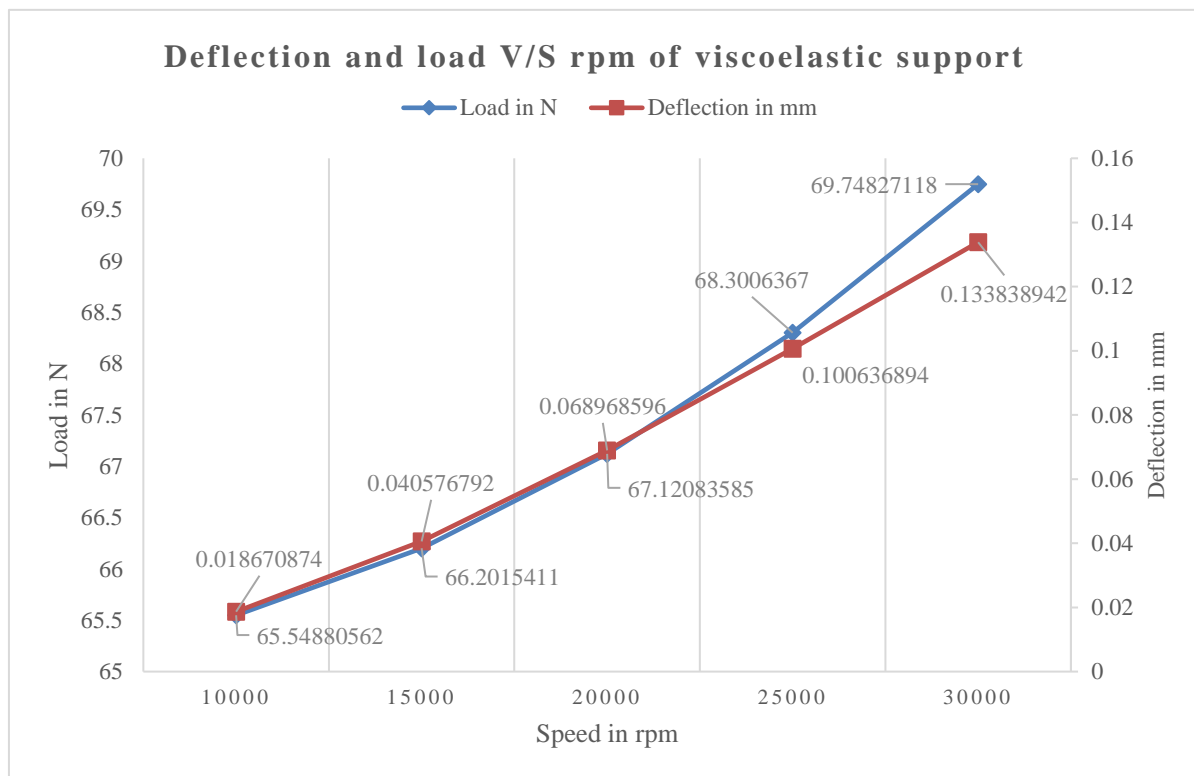


Figure 43 Sector angle 90-degree foil computed for viscoelastic support (Air Bubble)

We found that the maximum load on foil at 30k rpm is around 69.74N and the Deflection is 0.13 mm and also like the speed increase the deflection of foil and load on foil also increase as shown in the graph. Due to support, there is an improvement in load and the deflection also reduced when compared to previous models with no support.



Then we modeled the same configuration with 2 viscoelastic support (air bubble) in different positions to check if we get better results. The configuration is shown below.

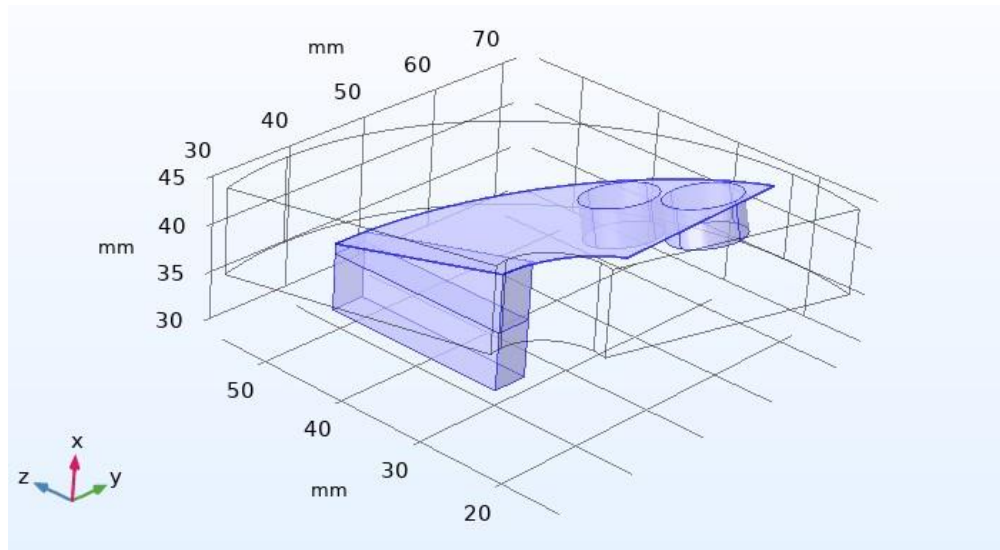


Figure 44 Model of 90-degree sector angle foil with 2 viscoelastic support (Air Bubble) Case 1

We found that the maximum load on foil at 30k rpm is around 70.12N and Deflection is 0.1186mm in 90-degree sector angle foil with 2 viscoelastic support (Air Bubble) Case 1 configuration. Then we again changed the position of the viscoelastic supports as shown below.

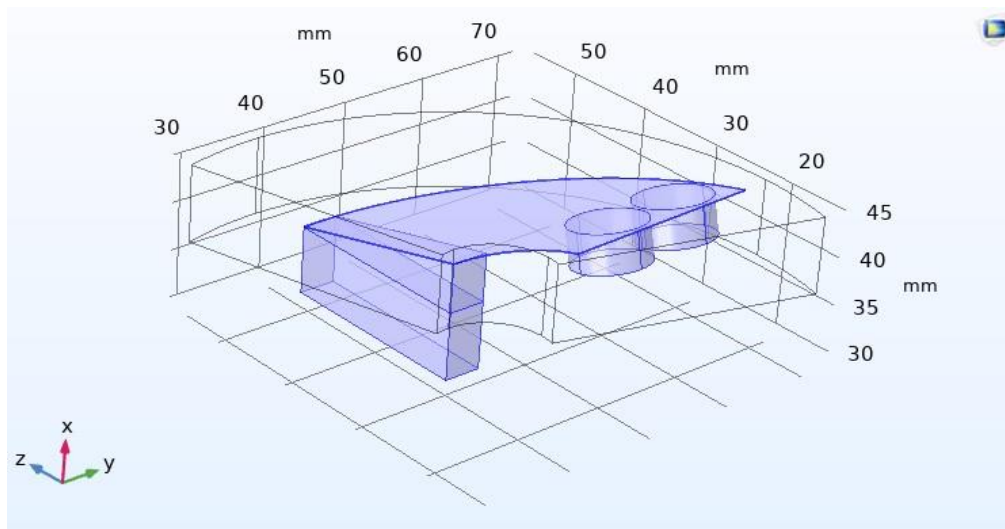


Figure 45 Model of 90-degree sector angle foil with 2 viscoelastic support (Air Bubble) Case 2



We found that the maximum load on foil at 30k rpm is around 70.13N and Deflection is 0.1048mm in 90-degree sector angle foil with 2 viscoelastic support (Air Bubble) Case 2 configuration. A slight increase in load and a decrease in deflection can be seen. Then we again changed the position of the viscoelastic supports as shown below.

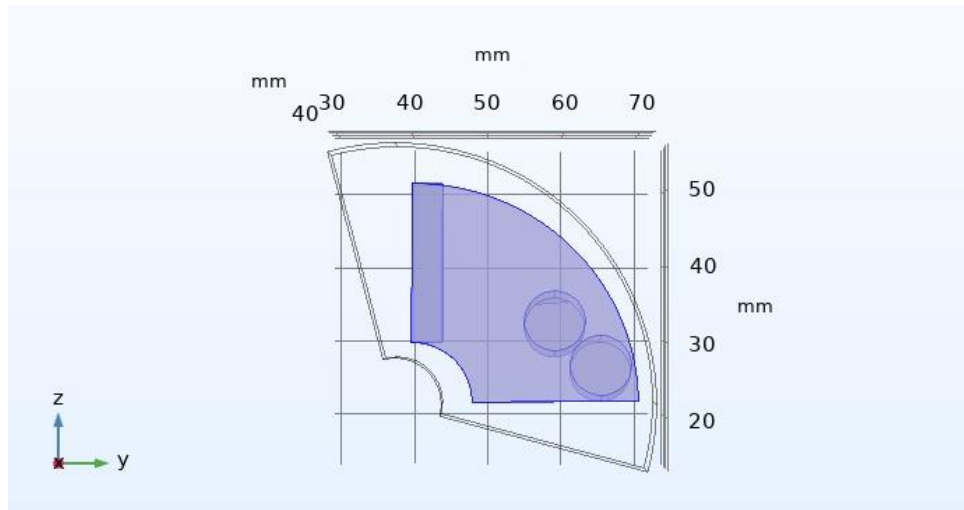


Figure 46 Model of 90-degree sector angle foil with 2 viscoelastic support (Air Bubble) Case 3

We found that the maximum load on foil at 30k rpm is around 69.66N and Deflection is 0.07896mm in 90-degree sector angle foil with 2 viscoelastic support (Air Bubble) Case 3 configuration. A slight decrease in load and a decrease in deflection can be seen. Then we again added 3 viscoelastic support as shown in the figure below.

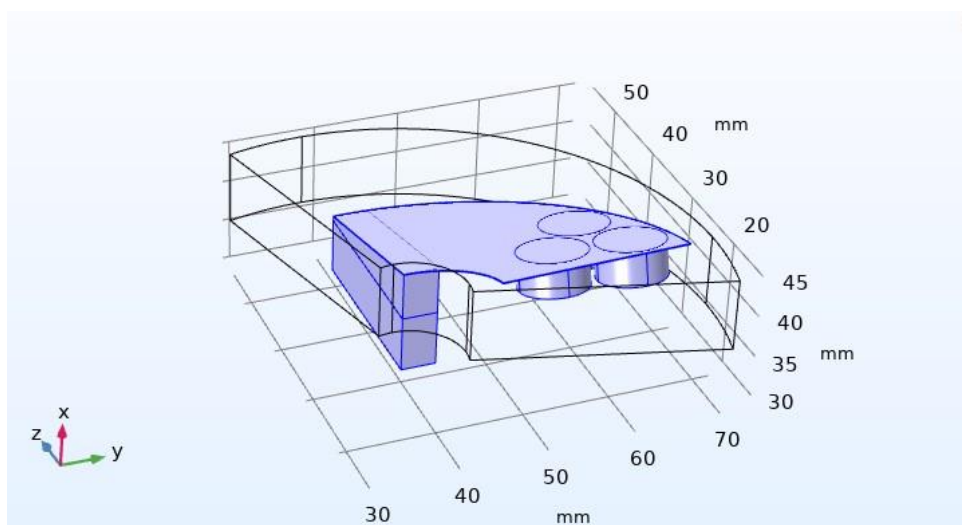


Figure 47 Model of 90-degree sector angle foil with 3 viscoelastic support (Air Bubble) Case 4

---

We found that the max load on foil at 30k rpm is around 69.9712N and the Deflection is 0.08024mm in 90-degree sector angle foil with 3 viscoelastic support (Air Bubble) Case 4 configuration. A slight increase in load and the increase in deflection can be seen. Now we got to know that providing more than one support we don't get max load so we decided to conclude.

In the viscoelastic configuration the 90-degree sector angle foil with 2 viscoelastic support (Air Bubble) Case 2 configuration we found that the maximum load on foil at 30k rpm is around 70.13N and Deflection is 0.1048mm. A slight increase in load and a decrease in deflection can be seen. This is the best maximum load-carrying capacity that was recorded and simulated when compared to all other configurations.

---

## **Chapter 10**

# **RESULTS AND DISCUSSION**

---

## 10. RESULTS AND DISCUSSION

The simulation of thrust foil bearing and its analysis was done. The designed model of a thrust foil bearing with 90-degree sector angle foil with 2 viscoelastic support (Air Bubble) Case 2 configuration gives maximum load-carrying capacity when compared with all other configurations we did before and 2 viscoelastic support (Air Bubble) Case 2 configuration foil thrust bearing model gives the best results for furthered researches.

Testing and simulations of thrust foil bearing were done by using COMSOL 5.0v Multiphysics software and the design was seen to be safe for running at 30k rpm with no problems and the maximum load-carrying capacity was around 70.13N. Stress distribution on foil shows stress concentration towards the trailing edge of the foil. The best results that we got from all configurations are shown below.

Table 4 Best results obtained from all configuration

Sl.no	Configuration	Load in N	Deflection in mm
1	Viscoelastic Support Case 2	70.13N	0.1048mm
2	Foil Thickness 0.5mm	67.19N	0.1594mm
3	90 Degree Sector Angle	65.20N	0.0285mm
4	60 Degree Sector Angle	48.61N	0.2179 mm
5	30 Degree Sector Angle	34.75N	0.0065 mm

---

The results obtained are in accordance with the FSI Simulation of the load-carrying capacity of thrust foil bearing. Hence, the maximum pressure region is found to be present in the region of convergence between the foil and runner.

Pressure distribution figures show that the pressure is maximizing towards the region of diminishing film height and there is maximum pressure near the tip of the foil. Pressure contour figures show that the pressure is maximum at the region of diminishing film height, due to the position of the film maximum pressure acts on that wall. Deflection figures show that the Displacement Field is maximizing towards the region of diminishing film height and there is maximum displacement near the tip of the foil (that is at the outer edge of the foil). Stress distribution figures show that the stress is maximum at the inner edge because more force acts on the inner edge due to the presence of support.

---

## **Chapter 11**

# **CONCLUSIONS**

---

## 11.CONCLUSIONS

This project has succeeded in its goal by providing a theoretical model to facilitate the design of thrust foil bearing. The conclusions of this preliminary work emphasize the importance of foil thickness, the number of foils, Sector angles of foil, and foil supports. An attempt has been made to conduct simulation and analysis in nature to obtain quantitative values of load carrying capabilities of thrust foil bearings as a function of different geometric and operating parameters.

Detailed analysis and simulations were studied and were conducted to evaluate the quantitative values of the load carried by the foil thrust bearing under dynamic conditions. Higher load carrying capabilities have been observed for foil thrust bearing having a higher number of supports to foils.

Future Scope, the results of this study show that beyond the specific foil design of a given bearing, several other factors can influence bearing performance. The further investigation includes varying foil material, changing the wedge area of foil, foil design, and using elastomers between foils. Continued work in this area is to develop more efficient AFTB with a higher load carrying capabilities.

---

## **Chapter 12**

### **REFERENCES**



---

## 12.REFERENCES

1. **Dr. Hooshang Heshmat** “Major Breakthrough In Load Capacity, Speed And Operating Temperature Of Foil Thrust Bearings” World Tribology Congress September 12-16, 2005, Washington, D.
2. **Quan Zhou, YuHou, Chunzheng Chen** “Dynamic stability experiments of compliant foil thrust bearing with viscoelastic support” Tribology International 42 (2008) 662–665
3. **Dykas, B.D.** “Design, Fabrication, and Performance of Foil Gas Thrust Bearings for Micro turbomachinery Applications. Volume 1: Aircraft Engine; Ceramics; Coal, Biomass and Alternative Fuels; Manufacturing, Materials and Metallurgy; Microturbines and Small Turbomachinery” [January], pp.629-639. 2008.
4. **Dykas, B.D. & Tellier, D.W.** “A Foil Thrust Bearing Test Rig for Evaluation of High-Temperature Performance and Durability “Technology, [April]. 2008.
5. **Park, D.** “Theoretical considerations of static and dynamic characteristics of airfoil thrust bearing with tilt and slip flow”. Tribology International, 41[4], pp.282-295. 2008.
6. **Dickman, J.R. & Prah, J.M** “AN INVESTIGATION OF GAS FOIL THRUST BEARING PERFORMANCE” Master of Science J.Iwan D. Alexander Paul Barnhart Chris Dellacorte Robert J. Bruckner. 2010.
7. **Yong-Bok Lee, Tae Young Kim, Chang Ho Kim & Tae Ho Kim**” Thrust Bump Air Foil Bearings with Variable Axial Load: Theoretical Predictions and Experiments” Tribology Transactions, 54: 902-910, 2011Copyright C \_ 2011 KIST.
8. **Franck Balducchi, Mihai” Arghir, Romain Gauthier, Emelyne Renard** “Experimental Analysis of the Start-Up Torque of a Mildly Loaded Foil Thrust Bearing” Journal of Tribology 2013 by ASME JULY 2013, Vol. 135 / 031702-1
9. **Tae Ho Kim, Tae Won Lee** “Design Optimization of Gas Foil Thrust Bearings for Maximum Load Capacity” Proceedings of ASME Turbo Expo 2015: Turbine Technical Conference and Exposition GT 2015 June 15 – 19.
10. **Luis San Andres, Keun Ryu, Paul Diemer.**” Prediction of Gas Thrust Foil Bearing Performance for Oil-Free Automotive Turbochargers” Journal of Engineering for Gas Turbines and Power Copyright VC 2015 by ASME.

- 
11. **Kai Feng, Liang-Jun Liu, Zhi-Yang Guo, and Xue-Yuan Zhao.**” Parametric study on static and dynamic characteristics of bump-type gas foil thrust bearing for oil-free turbomachinery” Proc IMechE Part J: J Engineering Tribology 0(0) 1–18! IMechE 2015.
  12. **Franck Balducchi, Mihai Arghir And Romain Gauthier** “Experimental analysis of the dynamic characteristics of a foil thrust bearing.” Journal of Tribology Copyright VC 2015 by ASME APRIL 2015, Vol. 137 / 021703-1
  13. **Yueqing Zheng, Tianwei Lai, Shuangtao Chen, Liang Chen, Liqiang Liu, and Yu Hou,** “Static characteristics of six pads multilayer protuberant foil thrust bearings” Proc IMechE Part J: J Engineering Tribology 0(0) 1–7! IMechE 2016.
  14. **Gen Fu, Alexandrina Untaroiu, Erik Swanson** “Effect of Foil Geometry on The Static Performance of Thrust Foil Bearings” Proceedings of ASME Turbo Expo 2017: Turbomachinery Technical Conference and Exposition June 26-30, 2017
  15. **Tianwei Lai, Yu Guo, Wei Wang** “Electro-hydrodynamic lubrication model of multi-decked foil thrust bearing with copper wire support” Journal of Mechanical Science and Technology 31 (9) (2017)
  16. **P Samanta<sup>1</sup> And Mm Khonsari,**” The Limiting Load-Carrying Capacity of Foil Thrust Bearings,” Department of Mechanical and Industrial Engineering, Louisiana State University, Patrick Taylor Hall, Baton Rouge, La 70803, USA 2017.
  17. **Travis A. Cable, Luis San Andres** “On the Design, Manufacture, and Premature Failure of a Metal Mesh Foil Thrust Bearing—How Concepts That Work on Paper, Actually Do Not” Journal of Engineering for Gas Turbines and Power DECEMBER 2018, Vol. 140 / 121007
  18. **Nguyen T. LaTray and Daejong Kim** “A HIGH-SPEED TEST RIG CAPABLE OF RUNNING AT 190,000RPM TO CHARACTERIZE GAS FOIL THRUST BEARINGS” Proceedings of ASME Turbo Expo 2018 Turbomachinery Technical Conference and Exposition GT2018 June 11-15, 2018, Oslo, Norway.
  19. **Kan Qin, Peter A. Jacobs, Joshua A. Keep, Daijin Li, Ingo H.** “A fluid-structure-thermal model for bump-type foil thrust bearings” Tribology International 121 (2018) 481–491.
  20. [https://en.wikipedia.org/wiki/Foil\\_bearing](https://en.wikipedia.org/wiki/Foil_bearing)
  21. [https://en.wikipedia.org/wiki/Thrust\\_bearing](https://en.wikipedia.org/wiki/Thrust_bearing)
  22. **Steve Bauman Glenn Research Center, Cleveland, Ohio** An Oil-Free Thrust Foil Bearing Facility Design, Calibration, and Operation

- 
23. <https://ntrs.nasa.gov/archive/nasa/casi.ntrs.nasa.gov/20050160253.pdf> An Oil-Free Thrust Foil Bearing Facility Design, Calibration, and Operation
  24. **Shan, X.C.** et al., A MICRO TURBINE DEVICE WITH ENHANCED MICRO AIR BEARINGS, Data Storage Institute, 5 Engineering Drive 1, Singapore 117608. Packaging [Boston, Mass.], pp.26-28. 2006.
  25. **Bauman, S.**, An Oil-Free Thrust Foil Bearing Facility Design, Calibration, and Operation. NASA/TM—2005-213568, 2005.
  26. INTRODUCTION TO TRIBOLOGY SECOND EDITION by Bharat Bhushan and the Howard D. Win Bigler Professor Director, Nanoprobe Laboratory for Bio- & Nanotechnology and Biomimetics The Ohio State University Columbus, Ohio USA – Text Book This edition first published 2013 John Wiley & Sons, Ltd